Dissertationes Forestales 227

Selection of training areas for remote sensing-based forest above-ground biomass estimation

Md Parvez Rana

School of Forest Sciences
Faculty of Science and Forestry
University of Eastern Finland

Academic dissertation

To be presented, with the permission of the Faculty of Science and Forestry of the University of Eastern Finland, for public criticism in the auditorium N100 of the University of Eastern Finland, Yliopistokatu 7, Joensuu, on September 2nd, 2016, at 12 o'clock noon.

Title of dissertation: Selection of training areas for remote sensing-based forest above-ground biomass estimation

Author: Md Parvez Rana

Dissertationes Forestales 227

http://dx.doi.org/10.14214/df.227

Thesis Supervisors:
Professor Timo Tokola
School of Forest Sciences, University of Eastern Finland, Joensuu, Finland

Dr. Lauri Korhonen
School of Forest Sciences, University of Eastern Finland, Joensuu, Finland

Pre-examiners:
Associate Professor Yousif Ali Hussin
Department of Natural Resources, University of Twente, The Netherlands

Professor Hannu Hyyppä
Department of Built Environment, Aalto University, Finland

Opponent:
Professor Markus Holopainen
Department of Forest Sciences, University of Helsinki, Finland

ISSN 1795-7389 (online)
ISBN 978-951-651-544-4 (pdf)

ISSN 2323-9220 (print)
ISBN 978-951-651-545-1 (paperback)

Publishers:
Finnish Society of Forest Science
Natural Resources Institute Finland
Faculty of Agriculture and Forestry at the University of Helsinki
School of Forest Sciences at the University of Eastern Finland

Editorial Office:
Finnish Society of Forest Science
P.O. Box 18 FI-01301 Vantaa, Finland
http://www.metla.fi/dissertationes

Rana MP. (2016). Selection of training areas for remote sensing-based forest above-ground biomass estimation. Dissertationes Forestales 227. 45 p. Available at http://dx.doi.org/10.14214/df.227

ABSTRACT

The aim of this work was to estimate forest above-ground biomass (AGB) – one of the fundamental parameters used in the forest inventory for measurement, reporting and verification (MRV) under the Reducing Emissions from Deforestation and Forest Degradation (REDD) and sustainable forest management (REDD+) mechanisms. In particular, this work examined the training area concept in a two-step approach for AGB estimation using airborne laser scanning (ALS) and RapidEye satellite data in the eastern area of Finland (Study I), the effect of the training area location (Study II), and the effect of sample size for the training area (Study III) using ALS, RapidEye and Landsat data in southern Nepal. The AGB model was fitted using simple linear regression (Study I) and the sparse Bayesian method (Study II-III). The AGB model performance was validated using an independent validation dataset, and the performance was evaluated by assessing the root mean square error (RMSE) and mean deviation. The findings of Study I show that the RapidEye model had a promising accuracy with a relative RMSE of 20% against an independent validation set. Study II findings showed that distance from road and the degree of slope in the training area had a considerable effect on the accuracy of the AGB estimation because the forest structure varied according to the level of accessibility. The findings of Study III indicated that an adequate coverage of the variability in tree height and density was an important condition for selecting the training areas. Only a minor increase in relative RMSE is observed when reducing the total number of training areas. ALS-based prediction required the smallest number of training areas when compared to the RapidEye and Landsat data. To conclude: (i) ALS-simulated training areas could be an alternative to expensive field sample plots using a two-step approach; (ii) the training area should cover a full range of variability in respect to accessibility factors and forest structures such as height, density; (iii) the ALS-based prediction outperformed RapidEye and Landsat data with reasonable accuracy. These evaluated concepts and issues of forest AGB inventory are likely to be useful in supporting future forest monitoring and decision making for the sustainable use of forest resources and REDD.

Keywords: Tropical forest, Nepal, LiDAR, RapidEye, Sample size, Carbon, REDD+, Boreal forest.

ACKNOWLEDGEMENTS

It is not always easy to acknowledge the debts that I have accumulated during the period of preparing this thesis paper. First of all, I am very grateful to Almighty Allah. I wish to express my gratitude and profound appreciation to the following, who in various ways, have contributed directly and indirectly to the completion of this study.

This thesis work has been conducted under the guidance of Professor Timo Tokola, to whom I would like to express my gratitude for his indispensable and expert guidance, suggestions, constructive criticism, encouragement and inspiration throughout the progress of this work. I would like to thank all of colleagues of University of Eastern Finland, especially Tarit Kumar Baul, Ashraful Alam, Kamrul Hassan, Yeasinur Rahman. I would like to give special thanks to Professor Sorin Popescu, Texas A&M University, USA where I spent six months as an exchange PhD student. Thanks also goes to all friends (especially Sajib Saha) and colleagues of College Station, USA.

I also express sincere gratitude to Tuomo Kauranne, and Jarno Hämäläinen, Arbonaut, Finland to give me permission to work on their LAMP (LiDAR Assisted Multisource Program) project, Nepal. Thanks also goes to Katja Gunia, Basanta Raj Gautam, Jussi Peuhkurinen, Katri Tegel, Petri Latva-Käyrä (Arbonaut Ltd). I also highly acknowledge to the authority of Forest Resource Assessment (FRA) project, Nepal who gave me permission to use project data for research purposes.

I express my deepest sense of gratitude to my parents and other family members because all my academic achievements are the outcome of their sacrifice, especially my elder brother (Golam Faroque) who always gives me a lot of inspiration, and encouragement to study hard from my childhood. Last but not least, I must express my gratitude to my wife Munira Yasmin for her love, dream, motivation, encouragement and also patiently sacrificed priceless time for my personal academic career.

This doctoral work was funded by the Finnish Cultural Foundation, Centre for International Mobility (CIMO), Graduate School in Forest Sciences (GSForest) and School of Forest Sciences, UEF. I appreciate their financial support.

Cheers
Md Parvez Rana
Joensuu, 2016

LIST OF ORIGINAL ARTICLES

This thesis is based on the following articles which are referred in the text by their Roman numerals (i.e. Study I, II, III). The articles are reprinted here with the kind permission of the publishers.

I Rana M.P., Tokola T., Korhonen L., Xu Q., Kumpula T., Vihervaara P., Mononen L. (2014). Training area concept in a two-step biomass inventory using airborne laser scanning and RapidEye satellite data. Remote Sensing 6: 285–309. http://dx.doi.org/10.3390/rs6010285

II Rana M.P., Korhonen L., Gautam B., Tokola T. (2014). Effect of field plot location on estimating tropical forest above-ground biomass of Nepal using ALS data. ISPRS Journal of Photogrammetry and Remote Sensing 94: 55–62. http://dx.doi.org/10.1016/j.isprsjprs.2014.04.012

III Rana M.P., Gautam B., Tokola T. (2016). Optimizing the number of training areas for modeling above-ground biomass with ALS and multispectral remote sensing in subtropical Nepal. International Journal of Applied Earth Observation and Geoinformation 49: 52–62. http://dx.doi.org/10.1016/j.jag.2016.01.006

Md Parvez Rana is the main and corresponding author for all three papers and responsible for the field and remote sensing data processing, analysis, calculation and composition of the papers, except for the field measurements. Professor Timo Tokola contributed to the thesis in terms of research idea development, supervision and guiding the first author. Mr. Basanta was responsible for field measurements and remote sensing data acquisition in Nepal. All co-authors contributed in writing and improving the peer-review articles.

TABLE OF CONTENTS

LIST OF ABBREVIATIONS

AGB	Above-ground biomass
REDD	Reducing Emissions from Deforestation and Forest Degradation
MRV	Measurement, reporting and verification
ALS	Airborne laser scanning
NDVI	Normalized difference vegetation index
ARVI	Atmospherically resistant vegetation index
NIR	Near infrared
OLS	Ordinary least squares
RMSE	Root mean square error
DTM	Digital terrain model
BRDF	Bi-directional reflectance distribution function
r^2	Coefficient of determination
SB	Sparse Bayesian
BIC	Bayesian Information Criterion
CHMs	Canopy Height Models

1 INTRODUCTION

1.1 Background

The Reducing Emissions from Deforestation and Forest Degradation (REDD+) concept is, at its core, a proposal by which developing countries may receive financial benefits for reducing emissions from deforestation and forest degradation, as well as forest conservation, changing the trend of the decreasing amount of forest biomass, and pursuing the sustainable management of forests and the enhancement of forest carbon stocks. The United Nations Framework Convention on Climate Change (UNFCCC) created the REDD+ mechanism to quantify and value the carbon storage services that forests provide. However the big challenge in successfully implementing this program is the measurement, reporting and verification (MRV) of forest carbon stocks (e.g. Næsset el al. 2016). Therefore, an important issue is how forest carbon stocks may be reliably predicted at a sub-national and national level.

Successful MRV for REDD+ is still a long way off. In the process of developing national REDD+ MRV frameworks, donors and policymakers have concentrated on cost information in order to develop strategies, to allocate budgets and to assess the effectiveness of forest carbon stock assessment (Wertz-Kanounniko 2008). The main limitations to the implementation of REDD+ have been institutional as well as financial, regarding the transaction and implementation costs for carbon credits (Murdiyarso et al. 2006). Transaction costs arise from the needs for prior information, and those emanating from the economic exchange itself (e.g. contract management, financial management, standard evaluation, technical assistance). Implementation costs are associated with the actions to reduce deforestation, forest degradation, to promote the sustainable management of forests and to enable the enhancement of forest carbon stocks (White and Minang 2011).

The current carbon stock in the world's forest is estimated to be 861 ± 66 Pg C where a tropical forest stores approximately 55% of the total carbon. Tropical forests have 56% of their carbon stored in biomass and 32% in soil (Pan et al. 2011). However, tropical deforestation has produced significant gross carbon emissions of 2.8 ± 0.5 Pg C per year. In addition, the Intergovernmental Panel on Climate Change (IPCC) has mentioned that deforestation and forest degradation contributed 10% of the total anthropogenic C emissions in their fifth assessment report (IPCC 2013). As a consequence, the net loss of carbon from tropical forests of around 1.1 ± 0.7 Pg C per year, despite a carbon sink by tropical growth forests of 1.7 ± 0.5 Pg C (Pan et al. 2011).

Describing and quantifying forest above-ground biomass (AGB) over a variety of spatial scales is a task of increasing importance (e.g. Tian et al. 2012). The prediction of AGB can provide critical information for quantifying the amount of carbon sequestered, guiding sustainable forest management, estimating the productivity of forest ecosystems, and creating greenhouse gas inventories (e.g. Lu 2006, Tian et al. 2012). Forest AGB could be estimated by field-based sample survey alone. However, field training data collection is the most expensive, time consuming part of forest inventory, especially in tropical forest due to issues of inaccessibility, and a complex heterogeneous forest with steep mountainous terrain. Therefore a combination of remotely sensed data and ground survey data can potentially offer a suitable means of monitoring, reporting and verifying forest AGB in a feasible and cost-effective way (Streck and Scholz 2006).

1.2 Alternative above-ground biomass prediction method

The selection of the prediction method plays an important role in remote sensing-based forest inventory. Both parametric (e.g. ordinary least squares) and non-parametric (e.g. *k*-MSN) methods are commonly used. The parametric approach has been widely used for the estimation of forest characteristics (e.g. Næsset 2002, Korhonen et al. 2008, Hou et al. 2011, Næsset et al. 2016). The main idea of this approach is to develop a linear relation between a dependent variable and one or more independent variables. The non-parametric approach is nowadays also widely used as an alternative to the parametric approach. Non-parametric imputation is defined as replacing missing values for any unit in the population with measurements drawn from another unit with similar characteristics (Temesgen 2003). The fundamental idea of non-parametric imputation is to locate the closest neighbor for the stand that does not have the tree-list information (target stands) from a pool of stands that have detailed tree and stand data (reference stands) (LeMay and Temesgen 2005, Temesgen 2003). Non-parametric imputation can retain attribute variance structures of the data, and so there is no assumption of distributional characteristics for either the auxiliary variables or the variables of interest (Moeur and Stage 1995, Katila and Tomppo 2002).

1.3 Airborne laser scanning-based forest inventory in tropical and boreal forests

Airborne laser scanning (ALS) is a remote sensing technology with a huge potential to increase accuracy and reduce costs in large-scale forest inventories (Asner et al. 2012, Næsset et al. 2016). Either wall-to-wall mapping or strip-based sampling can be used, both of which are established practices (Frazer et al. 2011). There are two main approaches to the interpretation of ALS data: the area-based approach (e.g. Næsset 2002) and individual tree detection (e.g. Vauhkonen et al. 2010). Stand-level forest inventories for large-scale applications are usually conducted using the area-based method (Næsset 2002, Maltamo et al. 2011). In this method, field-measured data and ALS metrics are used to develop an empirical relationship between the ALS metrics (used as predictors or independent variables) and a field-measured variable of interest (e.g. height and volume). Finally, these relationships are applied to obtain estimates of the target variables for the whole area of interest (Gobakken and Næsset 2009).

Several forest inventory parameters have been predicted with differing levels of accuracy in regard to ALS-derived variables, including AGB (Zhao et al. 2009). However, the application of ALS data for forest inventory is typically dependent on several parameters, including sampling design, plot size and location, sample density, estimation method, position error, and sensor characteristics (e.g. point density, flight altitude, footprint diameter and scan angle).

In both tropical as well as boreal forests, ALS-based forest AGB prediction is a task of increasing importance due to higher requirements for estimation accuracy, as well as the need to reduce the cost of large-scale forest inventories. A large number of ALS-based studies have been reported from all over the tropical region in recent decades (e.g. Drake et al. 2002, 2003, Lefsky et al. 2002a, 2002b, Asner et al. 2009, Hou et al. 2011, Næsset el al. 2016). Such an approach is feasible because wall-to-wall ALS achieves even the higher accuracy standards which are needed to ensure reliable estimates of carbon stocks and stock changes over time (Asner et al. 2012). ALS-based forests AGB prediction in tropical forests are not completely similar to boreal forests because of the forests characteristics and environmental

conditions. ALS-based forests prediction in tropical forests have lower level of accuracy compared to the boreal forests. Tropical forests are heterogeneous characterized by the greatest diversity of species with understory vegetation, while boreal forests are mostly homogeneous characterized by spruce, pine and birch with limited understory vegetation. Due to different characteristics of tropical forests and boreal forests, the thesis tested training areas development (see section 1.5) in Nepal as an example of tropical forests and in Finland as an example of boreal forests.

1.4 Optical data-based forest inventory in tropical and boreal forests

There are a multitude of optical remote sensing systems which are commonly employed for estimating forest attributes (e.g. AGB). Landsat image with a spatial resolution 30 m × 30 m has been employed in forest inventory from early era of remote sensing (see e.g. Næsset el al. 2016). The RapidEye image with a spatial resolution of 5 m has a good potential for use in several forestry operations, including cost-effective monitoring, and mapping, however there is relatively little evidence of its use in forest AGB estimation (see Englhart et al. 2012, Næsset el al. 2016). Lower relative RMSE values have been recorded in Scandinavian forests. However, the relative RMSE value has been seen to be higher in tropical forests due to the presence of dense forests with high understory vegetation. Næsset el al. (2016) reported a 63% of relative RMSE in miombo woodlands in Tanzania using RapidEye data. Moreover, Argoty et al. (2012) pointed out the importance of the red-edge band to quantify tropical forest AGB and also to detect forest degradation. RapidEye data might also be easier to obtain in many countries due to its relatively inexpensive price when compared to other remotely sensed data, such as ALS data. The drawback of all optical satellite images in the estimation of biomass is the saturation of predicted values in dense leaf canopies, which restricts estimates to low biomass levels (Garcia et al. 2010).

The most commonly used features derived from optical data to predict forest attributes are the spectral and textural features. Spectral features describe the tonal variation in portions of the electromagnetic spectrum. Textural features contain information about the spatial distribution of tonal variations within an image. Texture also has qualities such as periodicity and scale, and can therefore describe, for example, the direction, coarseness, and contrast of image components (Tamura et al. 1978). The combination of spectral and textural features has provided better levels of accuracy in the estimation of forest attributes than the use of any particular feature alone. Haralick et al. (1973) presented the use of grey-level co-occurrence matrices in quantifying the texture and their method has been widely used in remote sensing-based forestry applications (e.g. Tuominen and Pekkarinen 2005, Packalen and Maltamo 2007).

1.5 Training area concept and development

The training area in forest inventory refers the field sample area (plot) which is used to construct or calibrate statistical models. The calibrated model should able to tolerate possible any extremeness that could come from the validation stand. Therefore, the training area should foremostly cover the variability of the population (Montgomery et al. 2006, Frazer et al. 2011, Maltamo et al. 2011). To reduce the model bias, the training area can be either systemically distributed or completely random over the defined area. Different sampling

designs for training data collection have been evaluated, including random, systematic, cluster, strip, transect relascope, and adaptive cluster sampling. A well-designed sampling inventory can improve the effectiveness of field data collection and the precision of results. If random sampling is used to select the locations for training area collection, it may transpire that the sampled training data does not represent the entire population. Also, stratified sampling tends to reduce regression model prediction errors, ensuring that regression models do not extrapolate beyond the range of the training data (Hawbaker et al. 2009). Both Hawbaker et al. (2009) and Gobakken et al. (2013) concluded that the use of ALS data as prior information in the sampling design led to improved prediction accuracy. Maltamo et al. (2011) compared different methods for selecting training areas, including simple random sampling, stratified sampling based on forest type, stratified sampling based on geographic location, and stratified sampling based on ALS variables. They mentioned that if the training data failed to capture geographical trends in volume that reflected differences in site productivity and silvicultural practices, then the models might perform poorly for forest types that are inadequately represented in the sample. They therefore suggest that training areas should be located based on their geographic position if there is evidence of clear geographical trends.

Training areas are of further importance in forest inventory, especially in the context of tropical forest. The collection of training area may be expensive (sometimes accounting for a major portion of the total inventory cost), and can also be difficult to obtain depending on the forest conditions in the area of interest. Tokola and Shrestha (1999) mentioned that a problem in forest inventory optimization is in choosing the optimal sample design that maximizes the utility of data needs within certain budget constraints. In essence, training areas should cover the variability featured in the population, while simultaneously maximizing cost effectiveness. The correlation between the variables measured in the field and remote sensing variables should also be strong enough to provide substantial efficiency in terms of the model's predictive accuracy and the variation given a fixed number of training areas (Junttila et al. 2013). It is important to note that model efficiency can be defined on the basis of the number of field training areas required and their desired information content. It is therefore worth knowing which training models constructed using field data provide the most accurate and precise predictions with respect to cost and accuracy.

Due to the heterogeneous forest characteristics and different management regimes, it is necessary to have training area that is representative of both species distribution and forest characteristics. Also, access to the forest area may be difficult due to steep mountainous terrain. Therefore, a field campaign is challenging and is hampered by complex topographic conditions which increase labor efforts and costs. If only the most accessible areas were able to be used without any significant loss in accuracy, then major cost savings could be possible. However, these types of inventory designs may not capture the whole range of variability in the target forest structure. Thus it would be useful to have some guidelines on field sampling design to reduce the effects which are caused by the training area location (Dalponte et al. 2011). If the training areas are placed close together without covering the whole geographical region, then the cost of training data collection will be reduced, along with the needs for transportation or the entailment of significant walking distances. However, Maltamo et al. (2011) have noticed that the training area location may also affect the appropriateness of the regression models.

As a summary, the following factors should be considered when collecting field training area data: (i) the cost of the training data collection (Packalén et al. 2008); (ii) the total number of training areas (Gobakken and Næsset 2008); (iii) the sampling method utilized to

determine the distribution of the training area (Maltamo et al. 2011); (iv) ample coverage of the geographical variation in the forests (Maltamo et al. 2011); and (v) adequate coverage of the variation of vegetation characteristics (Junttila et al. 2013). Finally, an appropriate training area could lead to more accurate and precise growing stock estimates which could in-turn affect future management plans and decisions.

The estimation of forest AGB at national and sub-national scales is of growing interest throughout the world for quantifying the amount of carbon sequestered, guiding sustainable forest management, estimating the productivity of forest ecosystems, and creating greenhouse gas inventories. Focusing on the appropriate selection of training areas for forest AGB estimation (especially in context of tropical forests), this thesis tested following promising issues.

1.6 Objectives

The overall goal of this thesis was to estimate the AGB in tropical and boreal forests using active and passive remote sensing data. The specific objectives of the individual studies were:

Study I. To assess the training area concept in a two-step AGB estimation using ALS and RapidEye satellite data in boreal forests. To evaluate the accuracy of RapidEye-based prediction against the ALS-estimated sample plots (called surrogate plots) which were used as simulated ground-truth instead of more expensive field sample plots. To evaluate the accuracy of RapidEye-based prediction against an independent validation set.

Study II. To explore the effect of training area location on estimating tropical forest AGB in southern Nepal using ALS data. To test how the training area distance from road and the degree of slope can influence on the AGB prediction.

Study III. To optimize the number of training area for modeling AGB using ALS, RapidEye and Landsat data in southern Nepal. To evaluate the criteria to reduce the sample size for training area.

2 MATERIALS

2.1 Study areas

Two study areas were used in this thesis. Study Area I (Study I) is located in Finland (Figure 1), and Study Area II (Studies II-III) is located in Nepal (Figure 2).

Study Area I is situated in Kiihtelysvaara, in eastern Finland (62°31'N, 30°10'E). The boreal forests of the area are managed for timber production and ecological sustainability. Scots pine (*Pinus sylvestris* L.) is the dominant tree species, representing 73% of the volume. Norway spruce (*Picea abies* L.) represents 16% of the volume, and the remaining species come from deciduous trees such as downy birch (*Betula pubescens* Ehrh.) and silver birch (*Betula pendula* Roth.) which usually occur as minor species.

Study Area II is situated in the Terai Arc Landscape region (Terai and Siwaliks) of southern Nepal (between 27°14'N to 29°08'N, and 80°15'E to 85°49'E). Terai is situated in the south side of the study area and Siwaliks is in the north side of the study area. The region is a flat plain and the elevation ranges from 60 to 300 m. The region has a tropical to sub-tropical climate with the main tropical region being in the east, and drier areas in the west. Rainfall ranges from 600 mm in the west to 1300 mm in the east, with winter rain occurring in the west. This zone covers 22% of the total country's land mass (Pariyar 1998). The region is well-known for its productive, ecological and protective services, and also the secure livelihood that it provides for the surrounding people. The dominant tree species are Sal (*Shorea robusta*), Chir Pine (*Pinus roxburghii*), Schima (*Schima wallichii*), Axle Wood (*Anogeissus latifolia*), Marking Nut (*Semecarpus anacardium*), Karmal (*Dillenia pentagyna*), Indian Laurel (*Terminalia tomentosa*), Java plum (*Syzygium cumini*), Malabar Plum (*Syzygium jambos*), and Indian Gooseberry (*Phyllanthus emblica*).

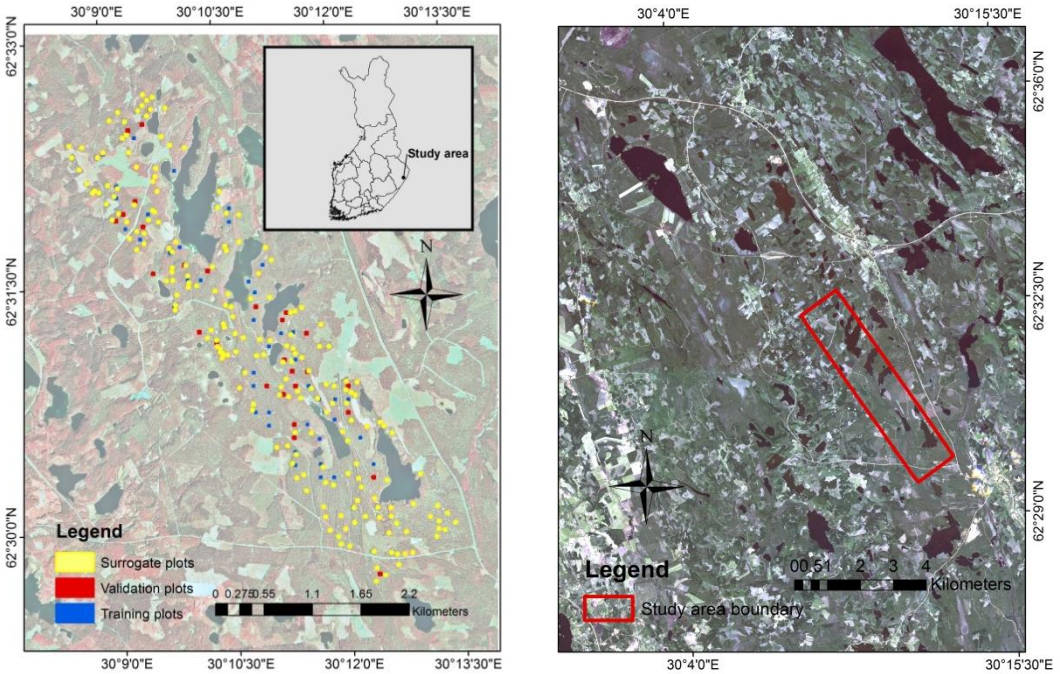

Figure 1. Training, surrogate and validation plots location and administrative map of Finland (left side), and RapidEye image with study area marked (right side).

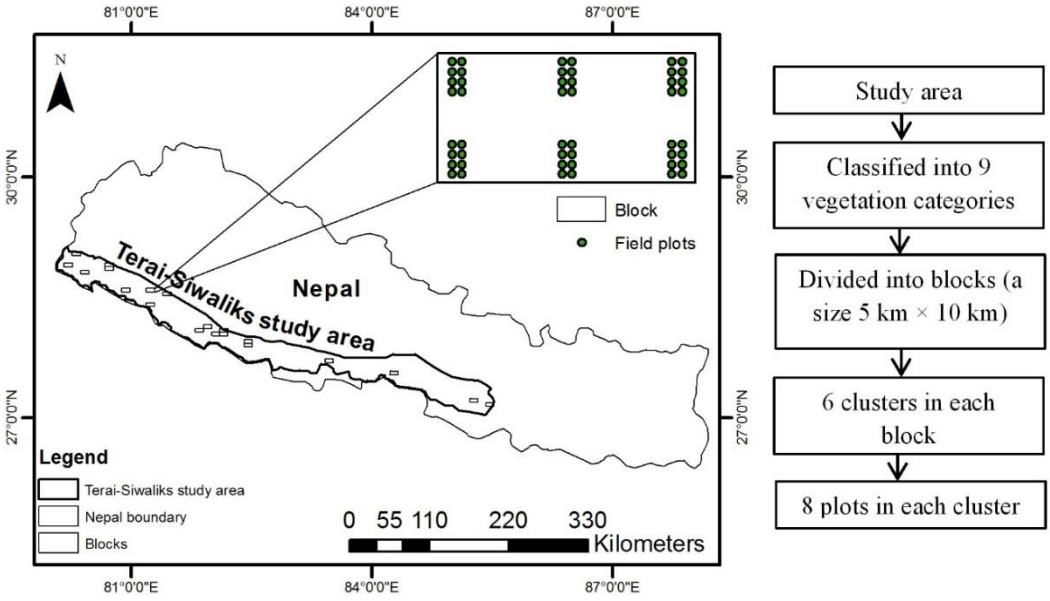

Figure 2. Left: Study area and location of blocks. One block is enlarged to demonstrate the design of field plots. Right: A sketch showing the sampling strategy.

2.2 Ground truth data

In Study I, the ground truth data were collected between May to June 2010. The study area is approximately 800 ha in the municipality of Kiihtelysvaara. Altogether, 78 field plots were placed subjectively into different stands in an attempt to record the species and size variation over the area. The field plots were placed based on the development class and dominant tree species. The sizes of the field plots ranged from 20 × 20 to 30 × 30 m. The field sample plots were divided into training (n = 50) (step I) and validation (n = 28) data sets, and the training set comprised of the plots whose size was 25 × 25 m (0.065 ha), and the other plots (with varying sizes) were used for validation. It is worth noting that larger sample plots maintain a greater amount of spatial overlap, minimize the edge effects, and increase the sample variances (Gautam et al. 2013). A total of 200 surrogate plots (35 × 35 m) were placed to cover the study area. These plots were used as a simulated ground-truth, and also while training the RapidEye models used in step II. The idea was that the surrogate plots should cover all of the variation (i.e. vegetation type, geographic location, species composition) seen in the study area. All trees with either diameter at breast height (DHB) ≥ 4 cm or height ≥ 4 m were measured in the field. The volumes of the individual trees were calculated as a function of DBH and tree height using species-specific models (Laasasenaho 1982). The AGB of individuals trees was calculated using the biomass equations developed by Repola (2008, 2009) for Scots pine, Norway spruce and deciduous. Finally, stem volume and AGB were calculated for each plot per hectare. The mean characteristics of the sample plots in the training (n=50) and validation (n=28) datasets are presented in Table 1.

In Study II-III, the ground truth data were collected between March 25th and May 20th, 2011. The field data were observed in two-stages. In the first stage, the whole study area (23 000 km^2) was classified into 9 vegetation categories utilizing the forest classification map

(30m resolution) developed by Joshi et al. (2003). The vegetation categories of the study area were hill-sal, sal, mixed, chir pine, riverine, degraded forest, grass, shadow and non-forest. The whole area was therefore divided into blocks (5 km × 10 km). Then a total of 20 blocks (1000 km^2) were chosen based on PPS (probability proportional to size) stratified sampling allocated randomly according to vegetation categories. Figure 1 shows the location of 20 blocks in the study area. In the second stage, a total of 632 field sample plots were surveyed in the blocks, and the coordinates of each plot center were recorded using a differential Global Positioning System (GPS). The locations of the field plots were selected using systematic cluster sampling within rectangular blocks. Each block contained six clusters, with eight plots in each cluster. The plots within a cluster were distributed in two parallel columns (from north to south) and in four parallel rows (from east to west). In Terai the distance between the column's and rows was 300 m. In Siwaliks, the column's distance was unchanged but the row distance was reduced to 150 m due to the high variation of the forests. The distance between cluster centers in the east–west direction was 3333 m, and in the north–south direction it was 2500 m. Tokola and Shrestha (1999) have previously found that there was little spatial correlation of ground truth plots within same cluster after 300 m in the Terai area and it was totally random after 350 m. Fixed circular plots (radius = 12.62 m) covering an area of 500 m^2 were utilized. Within each plot, the DBH of all living trees and shrubs thicker than 5 cm at breast height were measured using a diameter tape. Tree height was measured in the field for every 5^{th} tallied tree and the measured trees were used as a height sample tree. The heights of the remaining trees were estimated using species group specific height-diameter relationship with non-linear mixed-effect models. Power, Korf (1939) or Näslund (1936) functions were employed for non-linear mixed effect modelling depending on the species group. Power, Korf and Näslund growth functions were widely used functions for the development of standing volume and selecting an appropriate model form for each species, based on the height-diameter relationship. Finally, the stem volume and AGB of individual trees was estimated as a function of DBH, and tree height based on the species-species models presented by Sharma and Pukkala (1990). The plots were randomly divided into training and validation datasets. A set of 500 plots were allotted as training data and the remaining 132 plots were employed as validation data for testing the accuracy of the fitted models. The mean characteristics of the sample plots in the training (n=500) and validation (n=132) datasets are presented in Table 2.

Table 1. The mean characteristics of the ground truth data used in Study I.

	Minimum	Maximum	Mean	SD
Training plots, n = 50				
Stem volume (m^3/ha)	96.1	433.8	209.3	74.9
AGB (ton/ha)	51.5	226.6	113.0	39.7
Validation plots, n = 28				
Stem volume (m^3/ha)	103.6	382.5	219.1	69.0
AGB (ton/ha)	55.9	182.2	115.7	31.5

Table 2. The mean characteristics of the ground truth data used in Studies II-III.

	Minimum	Maximum	Mean	SD
Training data, n=500				
Height (m)	4.76	40.38	16.78	6.04
DBH (cm)	5.95	96.10	32.65	15.50
Stem density (n/ha)	20	2159	678	442
Basal area (m^2/ha)	0.10	50.55	16.93	8.97
Stem volume (m^3/ha)	0.40	526.28	142.67	95.74
AGB (ton/ha)	0.53	675.31	181.43	120.85
Canopy closure (%)	0.00	99.20	62.65	24.90
Validation data, n=132				
Height (m)	5.90	46.56	16.47	7.10
DBH (cm)	7.69	100.31	32.29	17.54
Stem density (n/ha)	20	2218	713	474
Basal area (m^2/ha)	0.21	41.48	16.84	9.22
Stem volume (m^3/ha)	0.83	375.87	139.68	94.07
AGB (ton/ha)	0.51	476.55	176.10	116.74
Canopy closure (%)	0.00	99.20	61.53	23.97

In Study II, in order to test the effect of the training area location, training and validation datasets were split into different sub-sections according to their distance to the road and slope. Table 3 describes the sample-plot design and the number of training and validation plots within each category. A total of 13 training plot location designs (SD1–13) were compiled. We used the same validation dataset (n=132) for testing all of the training plot designs. The sample plot distances to the road were determined using Nepal road layer (1996), Google Earth satellite imagery (2012) and ESRI's online World Street Map. The distance to the road was measured separately for each plot. The degree of slope of the sample plots was calculated using the Advanced Spaceborne Thermal Emission and Reflection Radiometer (ASTER) digital elevation model (DEM) (with a raster data of 30 m resolution). The degree of slope ranged between 0 and 40 degrees for both training and validation datasets, and the mean slopes were 9 (±9, SD) and 12 (±10, SD) respectively. The sample-plot distances to the road ranged between 0 and 14 km and the mean distances were 4 km (±3, SD) and 5 km (±4, SD) for the training and validation datasets, respectively.

Table 3. Sample-plot design for the study area (Study II).

Sample-plot design (SD)		Description	Number of Training plots	Number of Validation plots
1	D2	Sample plot located <2 km distance from road	169	38
2	D2–5	Sample plot located 2–5 km distance from road	199	41
3	D5+	Sample plot located >5 km distance from road	132	53
4	D5	A combination of D2 and D2–5	368	79
5	D25+	A combination of D2 and D5+	301	91
6	D2+	A combination of D2–5 and D5+	331	94
7	S10	Sample plot with <10 degrees slope	310	64
8	S10–20	Sample plot with 10–20 degrees slope	111	36
9	S20+	Sample plot with >20 degrees slope	79	32
10	S20	A combination of S10 and S10–20	421	100
11	S1020+	A combination of S10 and S20+	389	96
12	S10+	A combination of S10–20 and S20+	190	68
13	SD500	All sample plots	500	132

2.3 Airborne laser scanner data

For Study I, the ALS data were collected on 18th July 2009 using an Optech ALTM Gemini laser scanning system. The nominal pulse density was about 0.65 per square meter. The test site was scanned from an altitude approximately 2000 m above ground level with a field view of 30 degrees and side overlap between transects of 20%. The pulse repetition frequency was set to 50 kHz. The swath width was approximately 1,050 m.

For Studies II-III, the ALS data were collected during daytime between March 14th and April 2nd 2011 using a Leica ALS50-II laser scanning system operating at an altitude of 2200 m above ground level with a field view of 40°. The pulse repetition frequency was 52.9 kHz and the flying speed 80 knots, which resulted in a nominal pulse density of 0.8/m^2. The mean footprint diameter was 50 cm at ground level. A flight line overlap of 20% was utilized, and both first and last return data were recorded for each pulse.

2.4 Optical images

For Study I, the RapidEye satellite images were collected for the test area on 19th May 2012. RapidEye imagery provides multispectral optical imagery of five bands (blue 440–510 nm, green 520–590 nm, red 630–685 nm, red-edge 690–730 nm, and near infrared 760–850 nm). A total of two RapidEye images were collected with a spatial resolution of five meters to cover the study area. All of the RapidEye images were radiometrically and geometrically corrected (overall standard error was 0.53 m) according to the prescribed standard (RapidEye

2012) and aligned to a cartographic map projection. The RapidEye satellite orbit altitude was 630 km in a sun-synchronous orbit with a swath width of 77 km. The RapidEye image acquisition date was almost two years after the ground truth and ALS data acquisitions because of the unavailability of more concurrent data in the RapidEye archive. However, there were no harvesting and logging activities, or significant naturally occurring changes which had taken place within the target area during that time period.

For Study III, the RapidEye images were acquired between the 15th and 25th of March, 2011. Again, all RapidEye images were radiometrically and geometrically corrected and aligned with a cartographic map projection according to the RapidEye standards (RapidEye 2012). In addition, four Landsat 5 TM scenes were acquired. Each scene was a level 1T image (Standard Terrain Correction level) with a spatial resolution of 30 meters. The images were acquired in January and February of 2010 and 2011. The processing level included radiometric and geometric corrections based on ground control points and the available DTM (U.S. Geological Survey 2012).

3 METHODS

3.1 Preprocessing and predictors of airborne laser scanning

For all Studies, the ALS points were classified as ground and non-ground returns using the TerraScan tools following the methodology of Axelsson (2000). A digital terrain model (DTM) was created from the ground laser hits by subtracting the last return z-coordinates from the height measured via the geoid (grid spacing of 1 m). In addition, DZ values (distance-to-ground, also known as canopy height) were created by subtracting the DTM from that of the first and last returns using a ground model z factor of 0.001 (returns from the ground or from stones or shrubs less than 1 m in height were excluded from the model). The area-based method was used to model the relationships between the field-measured AGB and the ALS canopy metrics (Næsset 2002). The following ALS explanatory predictors (canopy height and density metrics) were calculated for sample plots to build AGB model:

- Height of the 10%, 20%, 30% … 100% percentile for first pulse points.
- Height of the 10%, 20%, 30% … 100% percentile for last pulse points.
- Mean height of first pulse high vegetation points (points over high vegetation threshold 5 m).
- Standard deviation of first pulse heights.
- Ratio of a measurement with a first pulse height less than 5 m to all first pulse height measurements.
- Ratio of a measurement with a last pulse height less than 5 m to all last pulse height measurements.
- Ratio of last pulse with a height less than 1.5 m + $i \times 3$ m for $i = 0...7$ and total number of last pulse.
- Logarithm of the measurement of the first pulse height less than 5 m to all first pulse height measurements.
- Mean of the largest three heights within the first and single echoes.

3.2 Preprocessing and predictors of RapidEye and Landsat

For Study I, a radiometric correction of the RapidEye image was unnecessary. We examined the necessity for radiometric correction based on histogram matching and the Ridge method (Song et al. 2001). We found that the slope and intercepts in the resulting feature space images were always one and zero respectively. For Study III, the RapidEye images were acquired on different dates and during different reflectance conditions, which affected the correlation with vegetation structure. The un-calibrated RapidEye images had anomalies due to differences in the properties of adjacent images caused by a bi-directional reflectance effect. Local radiometric calibration was therefore employed before any further processing could be done. Landsat 5 TM (Thematic Mapper) images were utilized as references because the effect of their bi-directional reflectance distribution function (BRDF) was negligible compared with that of the RapidEye images. The Landsat images were calibrated relative to each other utilizing the multiple linear regression approach presented by Tokola et al. (1999). Local radiometric calibration was performed on the RapidEye images utilizing the method developed by Tuominen and Pekkarinen (2004). The local adjustment was carried out separately for each RapidEye band (blue to blue, green to green, red to red, red-edge to red, and near infrared to near infrared). As Landsat does not have a red-edge band, the red band was used for that purpose.

For Studies I and III, in addition to the 5 m × 5 m raster of pixels of the five spectral RapidEye band values, a combination of vegetation indices and textural features were included in the AGB modeling (Table 4). Each plot extent was utilized to extract a subset image of the spectral bands, vegetation indices, and textural features. The image value associated with the pixel containing the plot center was associated with the forest attributes measured on the plot. In Study I, three normalized difference vegetation indices (NDVI) and 14 textural features (Haralick et al. 1973) were computed for the NIR-based NDVI and Red edge-based NDVI respectively. However, in Study III, two normalized difference vegetation indices (NDVI) and 14 textural features were computed using the NIR-based NDVI.

Similar to RapidEye data, the 30 m × 30 m raster of pixels of the six spectral band values were calculated, along with two vegetation indices from the Landsat TM images (Table 4). These included: (1) NDVI; and (2) the atmospherically resistant vegetation index (ARVI). The ARVI was calculated using the near-infrared, red, and blue bands as defined by (Kaufman and Tanre 1996).

Table 4. Spectral and textural features from optical data employed in Study I and III.

Sensor	Study I	Study III
RapidEye	Blue, Green, Red, Red-edge, NIR, NDVI, Haralick textural features	
Landsat		Blue, Green, Red, NIR, $SWIR_1$, $SWIR_2$, NDVI, ARVI

3.3 Sample size (n) for training area

In Study I and III, the effect of different sample size for the training areas was tested. A strategy of reducing the sample size was used to demonstrate the prediction accuracy when different numbers occur within training plots. We showed the prediction accuracy at different sample sizes, while maintaining the variation in the characteristics of the forest. This approach may be used to study how a representative field sample can be used in statistical prediction, and to identify when the number of training areas is too small. It can also allow for the prediction of an attribute within its value range with reasonable accuracy (a task which is useful for mapping purposes). We also explored the effect of a reduced sample size for each sensor i.e. ALS, RapidEye and Landsat (Study III). In Study I, the number of training plots was reduced from 50 to 25 and 10, based on the combination of tree height and AGB distribution.

In Study III, the sample size was reduced continuously, trimmed by 50 plot increments (e.g. 500 plots to 450 plots, ... down to 50 plots). The reduction of the sample size was done using systematic sampling in a feature space, based on two separate criteria such as (*i*) ALS metrics and (*ii*) the AGB distribution. When this sampling method is applied, we need to stratify the population (field plots) systematically in a feature space using ALS metrics and AGB distribution information. The fundamental goal of the systematic sampling is to provide equal chance (probability) of selecting each unit from within the population when creating the sample. This sampling involves firstly selecting a fixed starting point in the larger population, and then obtaining subsequent observations using a constant interval between samples. We first identified the required sample size. Then we divided the total number of the population by the sample size to obtain the sampling interval. The sampling interval may then be used as the constant difference between plots. For example, if a sample size of 50 is required, then we need to divide the total number of the population (n=500) with the sample size (n=50) to obtain a sampling interval of 10. Thence, we select every 10^{th} plot from the population.

In Study III, the fundamental goal of the ALS-guided approach was to maintain the range of values over the x- and y-axes so that the training plot set could cover the variation of the criteria of interest (in this case tree height and density). The ALS-guided strategy helps to capture the distribution of the population. The ALS-guided reduction of sample size was based on two ALS variables: the first pulse 80^{th} height percentile (H_{fp80}), and the vegetation ratio in the first pulse points (D_{fp}). The H_{fp80} were employed as the first criteria when sorting the training plots followed by the D_{fp}. Every n^{th} plot was then selected from the population according to the sample size. In the second set of reduction strategies, the training plots were arranged by field-measured AGB values in ascending order. A similar technique was then followed when selecting the training plots from the whole set.

In Study III, the number of field training plots was also approximated using two-phase sampling with a regression estimator and an assumption of a 10% standard error of the mean estimates. We used this to demonstrate how many training plots we would need if we collected the training plots using two-phases with a regression estimator and alternative remote sensing data with different correlations to the field information. We were willing to see how this two-phase sampling approximation would work in this situation (in our study area). The two-phase sampling formula provides the final number of plots needed when a statistically sound mean value for a specific area is of interest. The optimal number of field training plots (n_2) was based on the r^2 (coefficient of determination) values derived from field information and various remote sensing-materials, when specific mean accuracy is required

for a similar population. The formula for approximating the variance in population means (Eq. 1) was defined by (Köhl et al. 2006).

$$\hat{v}ar(\hat{\bar{Y}}_{2prgr}) = \frac{\hat{\mathrm{v}}\mathrm{ar}(y)(1-r^2)}{n_2} + \frac{r^2\hat{\mathrm{v}}\mathrm{ar}(y)}{n_1} - \frac{\hat{\mathrm{v}}\mathrm{ar}(y)}{N}, \quad \text{Eq. 1}$$

where $\hat{\mathrm{v}}\mathrm{ar}(y)$: approximation of the sample variance; N: total population; n_1: number of first phase sample; n_2: number of field training plots or second phase sample; and r^2: correlation between field-measured AGB and remote sensing-derived AGB. The total population (N) and the initial number of sample plots (n_1) can be very large because all of the image elements can be used during the first phase plots. Thus the last two terms can be ignored in the formula and it became Equation 2:

$$n_2 = \frac{\hat{\mathrm{v}}\mathrm{ar}(y)(1-r^2)}{\hat{v}ar(\hat{\bar{Y}}_{2prgr})} \quad \text{Eq. 2}$$

After determining the optimal number of training plots (n_2), we compared the cost of forest inventory in the context of each sensor using a sample market price. The cost of sensor data was 45€/km^2 for ALS, 1.05€/km^2 for RapidEye, and 0€/km^2 for Landsat. The cost of field data collection for a sample plot (500 m^2) was 300€/plot.

3.4 Above-ground biomass model construction

In Study I, the boreal forest AGB model was constructed in a two-step procedure using ALS and RapidEye data. Ordinary least squares (OLS) regression was used for the AGB model construction and an independent validation dataset was used for accuracy assessment. In step I, ALS data from 50 field plots were used to predict the AGB for the 200 surrogate plots. An AGB model was generated based on the relationship between ALS-metrics and field-measured training plots, and used to estimate the surrogate plots. In step II, the ALS-simulated surrogate plots were used as a ground-truth to generate a regression model between forest parameters (e.g. AGB) and features derived from RapidEye satellite imagery. The resulting RapidEye models were validated against an independent set of 28 plots.

In Study II-III, the sparse Bayesian (SB) method was employed to construct the AGB model. The sparse Bayesian method chooses a set of independent variables to form a model by giving weights to the explanatory variables (Junttila et al. 2008). The sparse Bayesian method assumes a normally distributed (Gaussian) likelihood function over the response vector, with a mean value of the independent variable and variance.

In all of the Studies, the final combination of predictors for building the AGB model was selected using a *regsubsets* algorithm. The selection criteria in the algorithm were the Bayesian Information Criterion (BIC) and the adjusted value of r^2. No explanatory variable having a partial *F* statistic with a significance level greater than 0.05 was left in the model during the predictor selection.

3.5 Accuracy assessment

In all of the Studies, the RMSE and relative RMSE (Eq. 3) were used for validating the accuracy of the forest AGB prediction. Mean deviation (Eq. 4) was also utilized for determining the accuracy of the model. In this context, mean deviation is the difference between the mean value of the model prediction and the corresponding plot observation.

$$\text{RMSE} = \sqrt{\frac{\sum_{i=1}^{n}(\hat{y}_i - y_i)^2}{\text{n}}},\ \text{RMSE}_{\%} = 100 * \frac{\text{RMSE}}{\bar{y}} \quad \text{and} \qquad \text{Eq. 3}$$

$$\text{Mean deviation} = \frac{\sum_{i=1}^{n}(\hat{y}_i - y_i)}{n}, \qquad \text{Eq. 4}$$

where y_i is the observed value and $\hat{y}_i$ the predicted value for sample plot *i*, $\bar{y}$ is the average value for the measured sample plots, and *n* is the total number of plots. The statistical significance of the mean deviation was estimated utilizing a *t*-test. The mean deviation was considered to be statistically significant if the absolute value of the *t* was greater than *t* corresponding with a probability of 0.05.

4 RESULTS

4.1 AGB model building and accuracy

In Study I, the AGB model accuracy was tested in a two-step procedure. In first step, the ALS models using all of the training plots (n=50) showed a promising accuracy with a relative RMSE of 17%. In the second step, the RapidEye models showed a relative RMSE of 20% against the ALS-simulated surrogate plots (n=200). When the RapidEye models were tested on independent validation plots (n=28), a relative RMSE of 20% was observed.

In Study II-III, the performance of the ALS, RapidEye and Landsat data for validation plots using all of the field training plots (n=500) is shown in Table 5. The results show that the ALS model provided the less error for validation plots using all the training plots, when compared to the RapidEye and Landsat data. The ALS data had the smallest relative RMSE (31%), followed by the RapidEye (52%) and Landsat data (53%).

In Studies II-III, the residuals of the sparse Bayesian models for validation plots using all training plots are matched against the fitted values in Figure 3. Although there were several outliers, these were retained in the models to help them tolerate possible model error (Hou et al. 2011). Statistical outliers were frequent in the RapidEye and Landsat models, which led to noise and non-constant variance in these cases. It can thus be said that the plot-specific standard error and standard deviation for the RapidEye and Landsat models did not fit with the data.

Table 5. ALS, RapidEye and Landsat-based above-ground biomass prediction for validation plots using all the training plots (Study I, n=50; Study II-III, n=500).

Study	Models	RMSE (ton/ha)	RMSE%	Mean deviation (ton/ha)	Adjusted r^2
Study I	ALS	18.7	16.6	0.0	0.766
	RapidEye	21.0	20.4	0.0	0.595
	RapidEye	23.6	20.4	–3.1	0.507
Study II-III	ALS	56.0	31.3	–3.8	0.768
	RapidEye	93.0	52.0	1.9	0.374
	Landsat	96.1	53.7	2.0	0.331

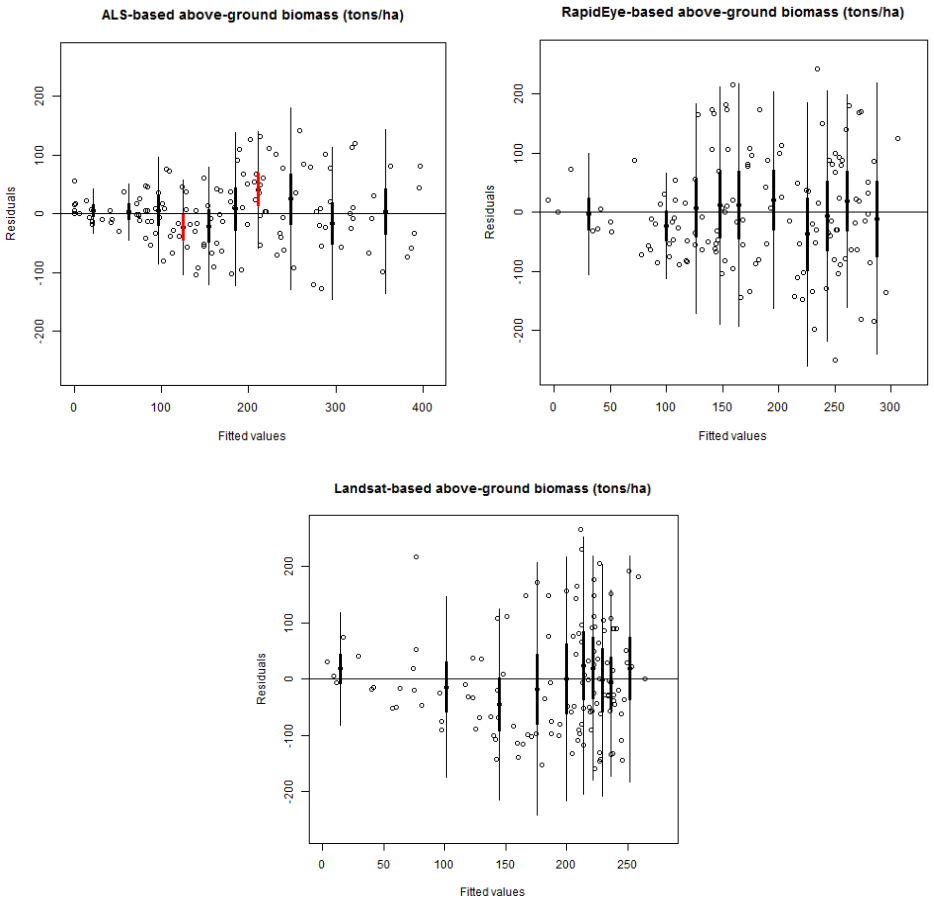

Figure 3. Residual plots of above-ground biomass (ton/ha). The thick lines show the standard error of the means and the thin lines the standard deviation (n=500 training plots).

4.2 Effect of training area location

In Study II, the results show that the effect of training plot location in the context of distance to road and slope had a considerable effect on the accuracy of the AGB estimation. The relative RMSE varied between 30-32% at the validation plot in all road distance categories (<2, 2-5, >5 km) (Figure 4). For all of the slope categories (<10, 10-20, >20 degree), the relative RMSE varied between 30-34% at the validation plot (Figure 5). Results shows that RMSE in slopes between 10–20 degrees is smaller than RMSE in slope between 0–10 degrees. The mean AGB value for training plots in the slopes between 10–20 degrees was 153 tons/ha (range 0.5–646 tons/ha), whereas it was 195 tons/ha (range 1–676 tons/ha) for 0–10 degrees. It could be one of the reason to report higher RMSE for 0–10 degrees slopes. However, the mean deviation was not significantly biased (α=0.05) for both categories plots. The single-sample *t*-test showed that the models for D5+ and S20+ were significantly biased (α=0.05), but the remaining training plot designs were not shown to be biased.

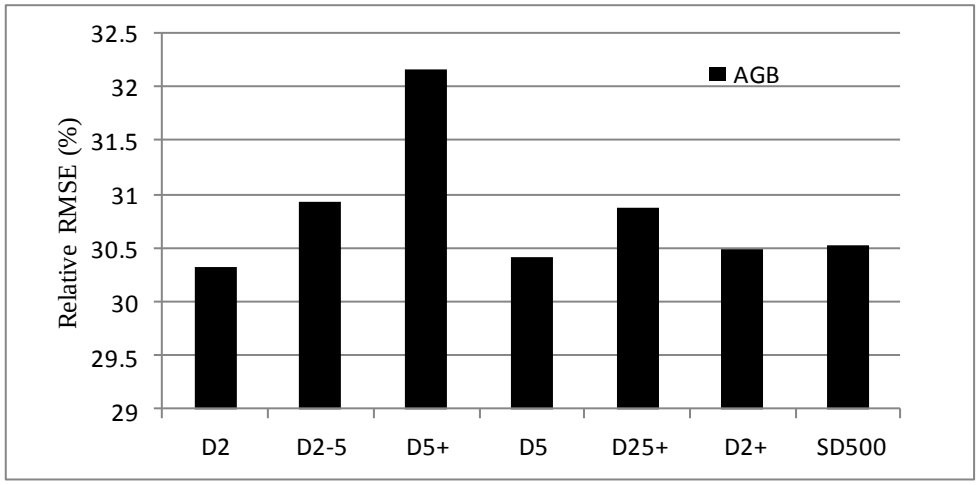

Figure 4. The relative RMSEs of AGB in distance to road based on training area location strategies. D2: <2 km distance; D2–5: 2–5 km distance; D5+: >5 km distance; D5: <5 km distance; D25+: <2 km and >5 km; D2+: >2 km distance; SD500: all the training plots.

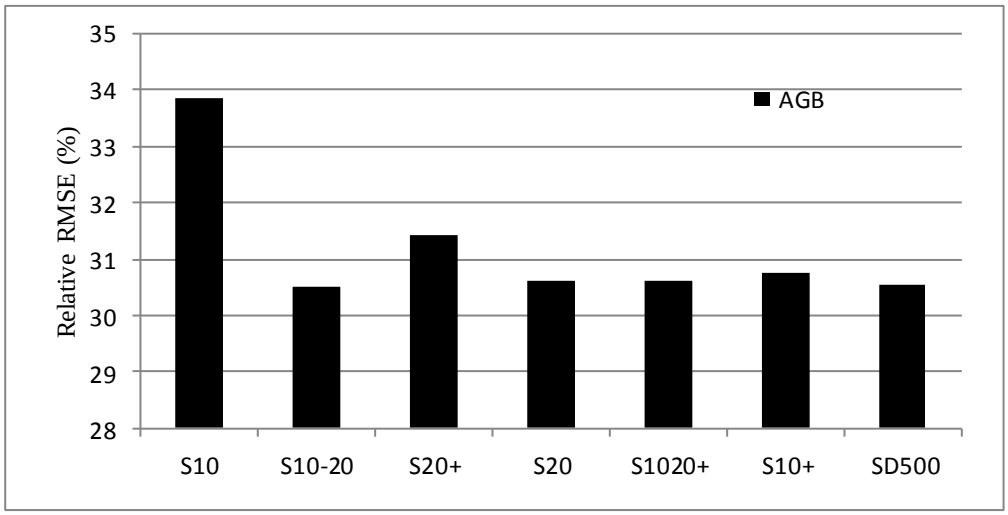

Figure 5. The relative RMSEs of AGB in slope categories based on training area location strategies. S10: <10 degrees; S10–20: 10–20 degrees; S20+: >20 degrees; S20: <20 degrees; S1020+: <10 and >20 degrees; S10+: >20 degrees; SD500: all the training plots.

4.3 Sample size (n) for training area

In Study I, the effect of sample size reduction was tested in a two-step procedure. In step I, the relative RMSEs for ALS-based AGB estimation were 17%, 20% and 12% when the sample size was reduced from 50 to 25 to 10 respectively. In step II, a relative RMSE of 20–21% for RapidEye-models were observed for all of the sample sizes (n=50, 25, 10) in both training plot and independent validation levels.

In Study III, the results indicate that the effect of the two sample size reduction criteria on the selection of training plots from the sample frame was prominent in the case of ALS-based AGB prediction, although the RapidEye and Landsat sensors failed to capture this effect. The predictive performance of the reduction criteria for ALS-based AGB prediction in terms of the relative RMSE is provided in Figure 6. ALS-guided sample size reduction had better accuracy compared to the AGB distribution-guided sample size reduction. The reduced number of sample size (450, 400,… 50) had a similar level of relative RMSE when all of the sample plots (n=500) were used.

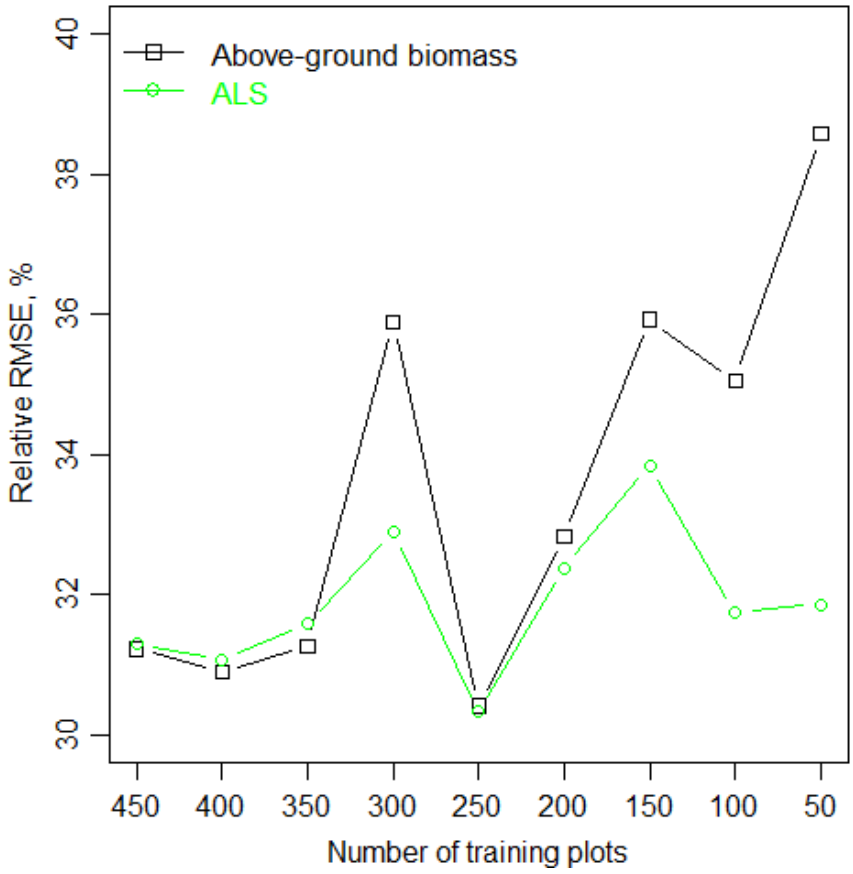

Figure 6. Relative RMSE of the ALS-based above-ground biomass estimate at reduced sample size. ALS: reducing the sample size based on ALS metrics; Above-ground biomass: reducing the sample size based on AGB distribution.

In Study III, the mean deviation for the sparse Bayesian-based AGB prediction at reduced sample size is shown in Figure 7. The impact of reducing the sample size on the mean deviation of the model prediction varied with the reduction criteria and degree of reduction. However, reducing the sample size based on the ALS metrics had less mean deviation than when based on AGB distribution. The use of fewer than 100 training plots resulted in a large mean deviation with both sample size and reduction criteria. AGB models were statistically significant ($\alpha = 0.05$) if the 100 and 50 training plots were selected utilizing the AGB distribution (Figure 7).

In Study III, the optimal number of training areas and associated cost of selected materials when employing a two-phase sampling approach with the assumption of a 10% standard error of the mean estimates are shown in Table 6 and Figure 8. ALS-based AGB estimation required the smallest number of field training plots, followed by RapidEye, and Landsat. Regarding the cost of data procurement, ALS-based inventory was shown to be cost-effective compared to RapidEye and Landsat alternatives (Figure 8).

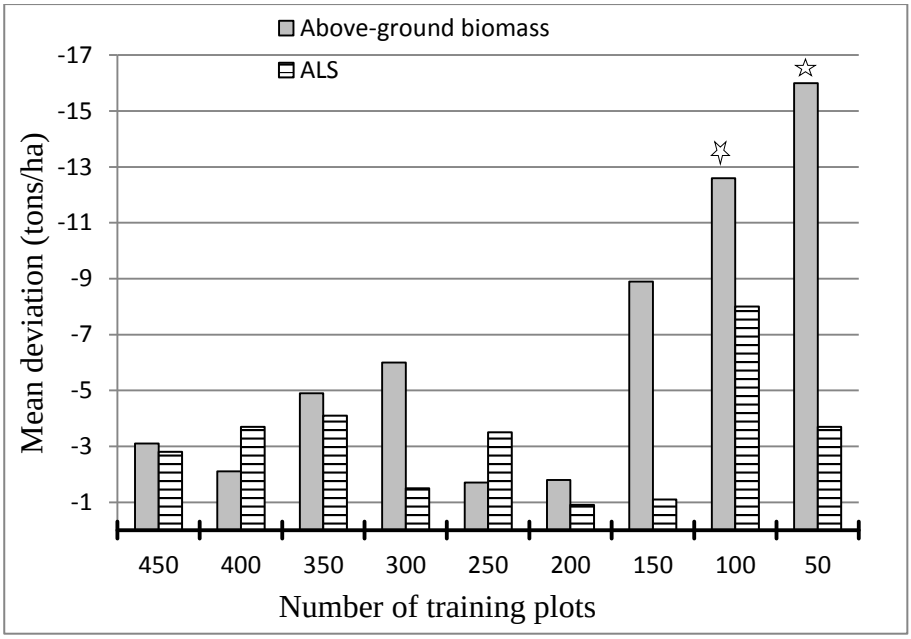

Figure 7. Mean deviation of ALS-based above-ground biomass estimates at reduced sample size. Above-ground biomass: reducing the sample size based on AGB distribution. ALS: reducing the sample size based on ALS metrics. The asterisks indicate that the model was statistically significant at α = 0.05.

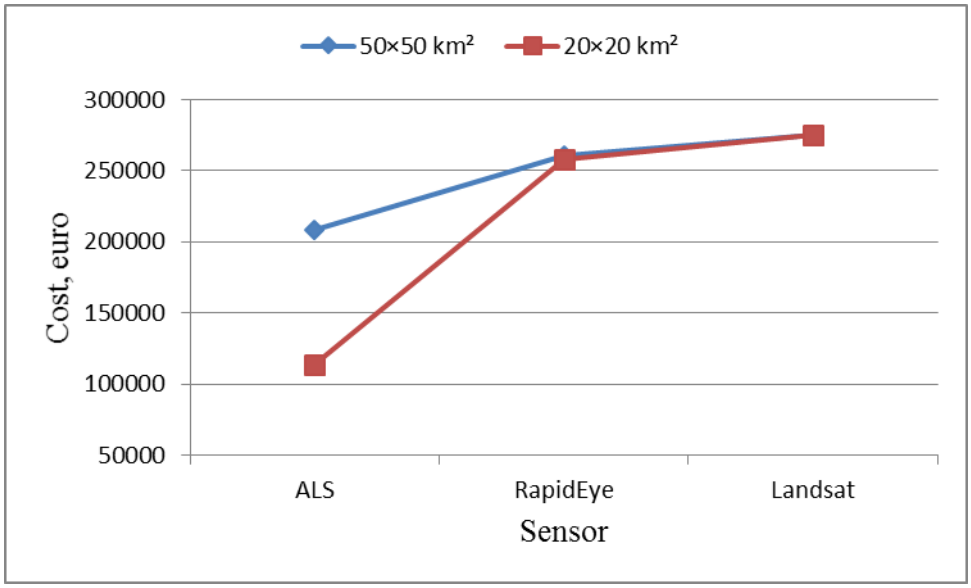

Figure 8. Comparison of ALS-, RapidEye- and Landsat-based forest inventory cost.

Table 6. Number of training areas required with different sensors according to the two-phase sampling approach when allowing for a 10% standard error of mean estimates.

Sensor	Adjusted r^2 of AGB	Number of field plots (n_2)
ALS	0.77	320
RapidEye	0.37	860
Landsat	0.33	918

5 DISCUSSION

5.1 Above-ground biomass model building and performance

In Study I, the overall strength of the ALS–RapidEye fusion revealed a promising accuracy to characterize AGB accounting in coniferous forest ecosystems. The analysis of linear regression showed that the ALS data had a good prediction accuracy at step I. Especially, it was promising that the ALS models explained 83% (r^2 value of 83%) of the variability for AGB. Furthermore, the RapidEye models provided a relatively good level of accuracy at step II. The RapidEye data had a relative RMSE of 20% at independent validation plots. Such accuracy indicates that the combination of ALS and RapidEye would be a promising fusion for the estimation of boreal forest attributes.

In Study II-III, the ALS-assisted AGB model for validation plots using all the training plots (n=500) resulted in a lesser level of error than either the RapidEye or Landsat models, and one promising feature was that it explained around 77% (r^2 value) of the variation. The resulting relative RMSE of 31% for the ALS-based AGB prediction is quite similar to previous studies (see Gonzalez et al. 2010, Clark et al. 2011). Such accuracy indicates that ALS has a good potential for predicting the attributes of tropical forests in the REDD+ program (Chambers et al. 2007, Asner et al. 2012). Koch (2010) has previously mentioned that the importance of ALS data is confirmed by a number of investigations which have repeatedly shown a higher performance of ALS data than other data types for estimating forest AGB.

In Study II-III, the comparative accuracy of the training and validation datasets showed that the validation data had lower RMSEs compared to the training dataset. Maltamo et al. (2011) noticed a similar trend of smaller RMSEs in the validation data than in the training data for the volume and stem count. The training dataset is often found to have a lower amount of estimation errors or RMSEs compared to the validation dataset (Dalponte et al. 2011, Hou et al. 2011). However, an opposite observation may indicate that there are either some outliers in the training data, or that the variance is smaller in the validation data. In this study, the sampling was not simulated, which makes this kind of result possible and corresponds with that of Maltamo et al. (2011). If the sampling was simulated (e.g. 100 times), then the average RMSEs would be closer to each other in both the training and validation datasets, and most probably, the average RMSE in the validation data would have been a little higher than the average RMSE in the training dataset. One reason for the relatively higher RMSEs seen in the training data is that the training data had a much higher

maximum volume and AGB values (Table 2). Also, the plots with a very high AGB may also be plots for which the estimates were quite poor.

5.2 Effect of training area location

In Study II, the effect of training area location strategies was tested in conjunction with the accuracy of predicting forest AGB. The relative RMSE, bias and bias probability were calculated for each strategy. The RMSE, bias, and bias probability varied significantly among the different categories of plot distance to road and also the degree of slope. The results showed that different training plot distances and slopes had a clear influence on the accuracy of the AGB estimation, and thus the forest structure in the study area was seen to vary in conjunction with its accessibility. Forests away from human settlements seem to be closer to their natural state, and therefore denser and more diverse. Thus, the training areas used for AGB modelling should cover the whole range of variability in regard to the distance to road and degree of slope. The heterogeneous characteristics of the Nepalese forests may however lead to a poorer model fit, and therefore affect prediction accuracies when several types of forests are merged into one model. Moreover, the spatial distribution of tree locations and tree size distributions may have an effect on estimation accuracy. Thus, the training data collection design should include information about accessibility factors. Tokola (2015) has also mentioned the importance of inaccessible areas to be included in the field protocol for remote sensing-based forest inventory. White et al. (2015) tested the training area location (i.e. slope) for ALS-based forest inventory attributes in a complex coastal forest environment. They indicate that ALS metrics and ALS-based forest attributes estimation (e.g. volume) were less varied across slope. Khosravipour et al. (2015) analyzed Canopy Height Models (CHMs) or normalized Digital Surface Models (nDSM) derived from ALS data to extract relevant forest inventory information. They suggested addressing the slope condition of individual trees or plots, especially in heterogeneous forest with multiple species or species which change their morphological characteristics as they mature. However, further testing must be performed with separate validation datasets in forests of different types.

5.3 Sample size for training area

The number of training areas is of great importance, as it accounts for the major proportion of inventory costs (Eid et al. 2004, Gobakken and Næsset 2009). The number of training areas should also be sufficient enough to cover the entire range of variability (tree species, tree size, site fertility etc.) in the forests of the inventory area (Gobakken et al. 2013). In general, the number of training areas needed for non-parametric methods should be more compared to those required for parametric methods. Unlike parametric methods, nonparametric methods make no assumptions about the probability distributions of the variables being assessed. The number of training plots featured in Study I and III were 50 and 500 respectively. We used an ordinary least square (parametric) approach in Study I, and the sparse Bayesian method in Study III (non-parametric).

In Study I and III, the sample size to estimate AGB using ALS, RapidEye and Landsat data were tested. Our results showed that only a minor increase in relative RMSE is observed when reducing the total number of training plots. Similar results have reported by Hawbaker et al. (2009), Maltamo et al. (2011), Dalponte et al. (2011), Gobakken et al. (2013), and

Junttila et al. (2015). The findings in Study III also revealed that ALS data successfully evaluated the strategy of minimizing the sample sizes compared to the RapidEye and Landsat. In addition, adequate coverage of the variability in tree height and density is an important consideration that should be addressed by the training plots which are selected (Study III).

Training areas are required to represent the characteristics of the whole forest area. Training areas which cover the variation of ALS height and density metrics enable us to obtain a model that is representative of the entire area, and thus provide a reasonable level of accuracy (Study III). For that reason, two ALS metrics correlated with tree height and density were used in reducing the sample size. These variables were expected to be a good choice for AGB prediction. However, some ALS variables will work better for certain forest inventory variables (e.g., basal area) than others. The selection of ALS metrics should therefore be based on the variable that needs to be predicted. Hawbaker et al. (2009), for instance, employed the mean and standard deviation of ALS heights when reducing their number of training areas in coniferous and deciduous forests.

In Study III, ALS-based AGB prediction required the smallest number of training areas, followed by RapidEye, and Landsat. A similar trend was seen for forest inventory cost (Figure 8). The number of training areas is generally dependent on the correlation between the remote sensing data and the training data. The traditional two-phase sampling approach provides a stable basis for estimating the optimal number of training areas (Tokola and Hou 2012). However, the present findings also show that the optimal number of training areas increases as the r^2 value between the field training data and remote sensing data decreases. Because of the high correlation, the number of training areas needed with ALS data was relatively small. The representativeness of the field training data and the presence of observations seen at the extremes of the value ranges are critical criteria when selecting field training information. Olofsson et al. (2014) mentioned that the number of training areas and the allocation of training areas in a REDD+ inventory should be based on the anticipated accuracy of the map and budget constrain, however the approach should ensure the scientific credibility of the results. Tuia et al. (2009) proposed two active learning algorithms for a semiautomatic definition of training samples in remote sensing image classification. They concluded that the required number of training samples can be reduced to 10%, reaching the same level of accuracy as larger data sets. This proposed method could be promising in a two-phase sampling process where a large number of low-cost first phase samples need to be taken from remote sensing images as an auxiliary variable.

5.4 Method pros and cons

In Study I, the forest AGB inventory method naturally places some advantages and constraints on the applicability of the method. In step I, the AGB inventory needed sample ALS data and requires only a few sample plots for model calibration (fitting). In addition, the surrogate plots (step II) could be placed systematically, by weighted random sampling or by stratified sampling over the whole area. Systematic sampling could be based on vegetation type, geographic location, climatic condition and tree species compositions. Traditional forest inventory depends on a large set of ground-truth data for model calibration, but the collection of field information is a main cost consideration. However, Study I showed a promising outcome where sample ALS data was employed as ground-truth data for model calibration, with a satellite image for mapping the whole area of interest. Our study showed that ALS-based forest inventory has produced very accurate estimates (step I). ALS data also

have a high accuracy to predict forest AGB when regressing ALS height/density metrics with data drawn from field measured plots. Subsequently, ALS estimates for the surrogate plots were used as simulated ground-truth (step II) for the interpretation of optical satellite images. This improved the results compared with using models that were directly based on the field plots. Covering the whole area of interest with ALS is relatively expensive, thus we used a two-step estimation approach that requires ALS data only for a sample of the study area. This is a so-called 'ALS-assisted multi-source program' that combines ALS information with field plots and satellite data to develop a forest resource map (e.g. Asner et al. 2011). Asner et al. (2011), Tokola (2015) also highlighted the use of ALS as an alternative to expensive ground sample data for large areas. Asner et al. (2011) also mentioned that the cost of ALS-assisted forest inventory along with satellite and field plot synthesis was $0.16 per ha compared to $1500 per ha for a solely field plot-based inventory. Wulder et al. (2012) concluded that ALS-plots can serve as calibration (fitting) and validation data (similar to ground plots) for modeling activities, or when sufficient forethought is given to design, they can support forest resources reporting. Nevertheless, more testing and validation should be done in different forest landscapes on a large-scale.

In Study I and III, another issue is that the satellite image acquisition dates may be different, thus introducing seasonal effects. Therefore, it would require the DN (digital number) values to be comparable between datasets which in turn would require the use of absolute reflectance instead of relative DN values. It would therefore be advisable to use the same season for image acquisition. In addition, the field data should always be collected during the same time period/season. In Study I, the RapidEye images were collected almost two years after the field and ALS data acquisitions. However, it was acceptable in our study because there were no harvesting and logging activities or significant naturally occurring changes within that time period. In addition, the focus points are typically spatial (e.g. generalization within an image or between images of different locations) and temporal (e.g. generalization between images of one location acquired over a period of time) (Tokola 2015). It is also important to focus on the complications arising from issues such as variation in the sensor used (e.g. a time series of fine spatial resolution data may comprise ALS, Landsat, RapidEye etc.), and in the sensor viewing (e.g. Korpela et al. 2010) and atmospheric conditions (e.g. Norjamäki and Tokola 2007, Xu et al. 2012).

Asner et al. (2012) evaluated a universal ALS approach for above-ground carbon estimation on regional and global scales in Panama, Peru, Madagascar and Hawaii. They were able to predict the above-ground carbon density using a single universal ALS model with an $r^2 = 0.80$, RMSE = 28 Mg C ha^{-1}. However, the bottleneck of their approach was the requirement of field basal area and wood density information in their final model. In general, the final model should be based only on explanatory variables derived from remotely sensed data. Häme et al. (2013) compared the linear regression analysis and probability method that combined unsupervised clustering and fuzzy estimation for AGB modeling. They mentioned that the linear regression analysis had a lower RMSE compared to the probability method. Vauhkonen et al. (2014) proposed a computational canopy volume (CCV) based on ALS data to improve predictions of forest AGB. A CCV is derived from ALS data based on computational geometry, topological connectivity and numerical optimization.

The integration of multisource data (e.g. sensor, topography, soil) to improve the AGB estimation accuracy should be refined because all sensors (e.g. ALS, radar) have their own positive and negative characteristics. Therefore, their proper integration can improve the AGB estimation accuracy (e.g. Walker et al. 2007). For instance, Mascaro et al. (2011) mentioned that ALS-derived above-ground carbon densities varied according to the slope

angle, forest age, bedrock and soil texture. This study also indicated that physiography may be more important in controlling above-ground carbon variation in Neotropical forests than is currently thought. In addition, Chen et al. (2012) have mentioned that the inclusion of vegetation type information derived from aerial photography could improve the statistical models. They reported a 10% reduction of RMSE for mixed-effects modeling when integrating ALS and vegetation types, compared to using ALS data alone. Lu et al. (2016) suggested two techniques for a better integration of different source data: (1) data fusion using certain techniques such as principal component analysis and partial least squares regression; and (2) the combination of different source data as extra bands.

5.5 Sensor pros and cons

The acquisition costs of remote sensing data and prediction accuracy are usually correlated (Tokola and Hou 2012). Hyyppä et al. (2000) also mentioned that the estimation error of the forest characteristics were smaller for higher resolution data compared to lower resolution data. In all of the Studies (I-III) we have shown that ALS is the most accurate remote sensing data, but has high acquisition costs, followed by RapidEye and Landsat data. Hou et al. (2011) also mentioned that ALS data can be a useful alternative to satisfy the demand for better accuracy, in spite of its high cost. ALS data enables the accurate three-dimensional characterization of vertical forest structure. ALS data does not suffer from saturation and is able to penetrate through even dense vegetation. Chambers et al. (2007), Asner et al. (2012) reported that ALS technology is fast turning the corner from a demonstration technology to a key tool for assessing highly dense tropical forests. Optical data however, conversely faces the saturation problem and an optical sensor records only the crown surface. This becomes a major issue when considering tropical forests which are highly dense with understory vegetation cover that often remains undetectable using optical satellite data.

A multitude of sensors with varying accuracy are currently being used for AGB estimation. Zolkos et al. (2013) conducted a meta-analysis of AGB estimation from 70 refereed articles using different remote sensing platforms (airborne and space-borne), and different sensor types (optical, radar, and lidar). The main focus of the study was on Lidar (Light Detection and Ranging) since these papers reported the highest accuracy when used in a synergistic manner with other multi-sensor measurements. They also highlighted the systematic differences in accuracy between different types of Lidar systems flown on different platforms, but perhaps more importantly, they highlighted differences between the forest types (biomes) and plot sizes used for model development and accuracy assessment. Häme et al. (2013) used optical data (ALOS AVNIR) and radar (ALOS PALSAR) data for AGB estimation in the tropical forest of Lao PDR. They mentioned that medium resolution AVNIR data was better than PALSAR data. However, a combination of mono-temporal AVNIR and PALSAR did not improve AGB estimation over the performance obtained with AVNIR data alone.

If the different sensors are compared for AGB modeling, one Lidar weakness is its relatively high cost. For radar data, the main issue is a temporal decorrelation when estimating forest AGB (Koch 2010). Temporal decorrelation is the modification of the interferometric coherence induced by changes of the target over time. Therefore tree height estimation from radar data becomes difficult, given that it is a basic input of forest AGB modeling. Optical sensors have difficulty managing a large amount of AGB (e.g. >150 ton/ha), although a major positive consideration is the availability for a time period of more

than the decades previous (e.g. Koch 2010). However the major challenge for all sensors is to achieve a more intensive development of integration models for multi-sensor data, with a requisite of new robust algorithms and statistical methods.

5.6 Statistical modeling

We used the OLS and the sparse Bayesian methods to predict AGB which are the most promising methods used in remote sensing-based statistical modeling. Penner et al. (2013) concluded that prediction accuracy and precision varied markedly with forest type, and no single statistical method produced results that were consistently superior. Næsset et al. (2005) concluded that employing a multivariate (multi-variable) method would not have any significant impact on the AGB estimation among the OLS regression analysis, seemingly unrelated regression (SUR) and partial least-squares (PLS) regression from two different inventories using ALS data.

In our studies, although the final combination of predictors for building the AGB model was selected using the *regsubsets* algorithm, Packalén et al. (2009) have mentioned that different predictor variables were identified during different runs of the automated variable selection method. For instance, Latifi et al. (2010), Packalén et al. (2012) reported that genetic algorithm (GA) and simulated annealing (SA) were also superior variable selection methods. These algorithms should nevertheless be tested as alternatives to see whether a different explanatory variable selection method would improve the result, or at least help to make the search for an eventual solution more effective. Regardless of this however, the ALS predictors (height and density metric) that we employed in the AGB models were closely matched to the predictors selected in other studies (e.g. Junttila et al. 2015). The RapidEye and Landsat spectral and textural features used in this study were also closely matched with those used in other studies (e.g. Packalén et al. 2007, Latifi et al. 2010).

5.7 Future prospects and visions

The REDD+ monitoring process will need good ground sample information for AGB estimation and forest area change detection, which extends over a time span. Although optical and radar data are only one tenth of the price of ALS, ALS data can be useful as ground-truth data for the estimation of large-area forest attributes (Tokola 2015). The potentiality of ALS to succeed within the REDD+ mechanism is its capability to penetrate through the dense canopy, and ALS response signal is good to detect changes in closed forests. ALS-based forest inventory will be feasible for operational REDD+ activities, however national or sub-national level forest inventory will only be cost-effective based on a combination of low-cost remote sensing data and ground sample information. Although remotely sensed data provides accurate information of forest AGB stocks for REDD+ activities, we still need to follow the good practices that are already in use in traditional forest inventories (Olofsson et al. 2014, Tokola 2015).

Payment for maintaining forest carbon stocks has significant potential to provide a cost-effective mechanism for climate change mitigation (Merger et al. 2012). Merger et al. (2012) indicate that the use of bottom-up approaches to estimate REDD+ economics by considering regional variations in economic conditions and carbon stocks has been shown to be an appropriate approach to provide policy and decision-makers with robust economic

information on REDD+. UNFCCC (2009) also suggest that policy has to stem from both local and national levels. Zahabu (2008) mentioned that REDD+ monitoring through an expert team is costly and such resources are scarcely available. Therefore, the involvement of local people in the monitoring and reporting stages will reduce the cost of implementing the REDD+ mechanism. Olofsson et al. (2014) also recommend following a process which employs the three major components including sampling design, response design (e.g. source of reference data, defining agreement, spatial assessment unit), and analysis (e.g. estimation accuracy) to develop a cost-effective REDD+ MRV. White et al. (2011) mention that regional training activities, regional MRV, regional independent monitoring, and the use of new technology (e.g. ALS) could reduce the transitional and implementation costs of REDD+ MRV.

There are number of new space missions anticipated which will be capable of providing high resolution images at an affordable price. Belward and Skøien (2015) mentioned that around 260 satellites with an Earth observation mission are either operating or planed over the next 15 years. Among the new remote sensing technologies, multispectral Lidar could be employed in forest biomass inventory. Multispectral Lidar could be capable of measuring both structural parameters (e.g. AGB) and physiological changes through the complete vertical extension of the canopy, including the understory. Such measurements can be precise, and achieve better estimates of the biodiversity and AGB associated with forests (Morsdorf et al. 2009, Woodhouse et al. 2011). Although airborne hyperspectral data have been widely used in investigating tree species classification (e.g. Pant et al. 2013), a combination with other remote sensing data could improve the accuracy for forest biomass and forest area estimation. In particular, tree species classification and leaf area information can play an important role as inputs for forest AGB estimation. For instance, Laurin et al. (2014) have already shown that the integration of hyperspectral bands ($r^2 = 0.70$) improved the model based on ALS alone ($r^2 = 0.64$) for AGB estimation in an African tropical forest. Forest AGB estimations using radar interferometry (extraction of height information) will therefore be an important step forward. In this respect, the radar tomography (the imaging of a three dimensional body using multiple two-dimensional slices) may also become a leading technological approach. The IceSat/GLAS system has recently been employed for forest AGB estimation, and is receiving more attention compared to other systems (Koch 2010).

As improvements in technology (e.g. multispectral Lidar, IceSat/GLAS) become available and new methods are developed, the REDD+ MRV will become progressively more effective. Also, regional MRV approaches, institutional capacity building, and the involvement of local people will help to facilitate the success of REDD+ MRV from international to local level. The study findings are likely to prove useful for not only REDD+ methodology development, but also in supporting automated forest biomass monitoring and enabling effective decision making for the sustainable use of forests resources.

REFERENCES

Argoty F., Cifuentes M., Imbach P., Vilchez S., Casanoves F., Ibrahim M., Vierling L. (2012). Quantification of forest carbon degradation in Nicaragua using RapidEye remote sensing data: El Cuá and Wiwili case studies. AGU fall meeting. http://adsabs.harvard.edu/abs/2012AGUFM.B41E0341A. [Cited 2 Feb 2016].

Asner G.P., Hughes R.F., Mascaro J., Uowolo A.L., Knapp D.E., Jacobson J., Kennedy-Bowdoin T., Clark J.K. (2011). High-resolution carbon mapping on the million-hectare Island of Hawaii. Frontiers in Ecology and the Environment 9: 434–439. http://doi.org/10.1890/100179

Asner G.P., Hughes R.F., Varga T.A., Knapp D.E., Kennedy-Bowdoin T. (2009). Environmental and biotic controls over aboveground biomass throughout a rain forest. Ecosystems 12: 261–278. http://doi.org/10.1007/s10021-008-9221-5

Asner P.G., Mascaro J., Muller-Landau H.C., Vieilledent G., Vaudry R., Rasamoelina M., Hall J.S., Breugel M.V. (2012). A universal airborne ALS approach for tropical forest carbon mapping. Oecologia 168: 1147–1160. http://doi.org/10.1007/s00442-011-2165-z

Axelsson P. (2000). DEM generation from laser scanner data using adaptive TIN models. International Archives of Photogrammetry and Remote Sensing 33: 110–111. http://doi.org/10.1016/j.isprsjprs.2005.10.005

Belward A.S., Skøien J.O. (2015). Who launched what, when and why; trends in global land-cover observation capacity from civilian earth observation satellites. ISPRS Journal of Photogrammetry and Remote Sensing 103: 115–128. http://doi.org/10.1016/j.isprsjprs.2014.03.009

Chambers J.Q., Asner G.P., Morton D.C., Anderson L.O., Saatchi S.S., Espirito-Santo F.D., Palace M., Souza C.J. (2007). Regional ecosystem structure and function: ecological insights from remote sensing of tropical forests. Trends in Ecology and Evolution 22: 414–23. http://doi.org/10.1016/j.tree.2007.05.001

Chen Q., Laurin G.V., Battles J.J., Saah D. (2012). Integration of airborne lidar and vegetation types derived from aerial photography for mapping aboveground live biomass. Remote Sensing of Environment 121: 108–117. http://doi.org/10.1016/j.rse.2012.01.021

Clark M.L., Roberts D.A., Ewel J.J., Clark D.B. (2011). Estimation of tropical rain forest aboveground biomass with small-footprint lidar and hyperspectral sensors. Remote Sensing of Environment 115: 2931–2942. http://doi.org/10.1016/j.rse.2010.08.029

Dalponte M., Martinez C., Rodeghiero M., Gianelle D. (2011). The role of ground reference data collection in the prediction of stem volume with ALS data in mountain areas. ISPRS Journal of Photogrammetry and Remote Sensing 66: 787–797. http://doi.org/10.1016/j.isprsjprs.2011.09.003

Drake J.B., Dubayah R.O., Clark D.B., Knox R.G., Blair J.B., Hofton M.A., Chazdon R.L., Weishampel J.F., Prince S. (2002). Estimation of tropical forest structural characteristics using large-footprint lidar. Remote Sensing of Environment 79: 305–319. http://doi.org/10.1016/S0034-4257(01)00281-4

Drake J.B., Knox R.G., Dubayah R.O., Clark D.B., Condit R., Blair J.B., Hofton M. (2003). Above-ground biomass estimation in closed canopy neotropical forests using ALS remote sensing: factors affecting the generality of relationships. Global Ecology and Biogeography 12: 147–159. http://doi.org/10.1046/j.1466-822X.2003.00010.x

Eid T., Gobakken T., Næsset E. (2004). Comparing stand inventories based on photo interpretation and laser scanning by mean of cost-plus-loss analysis. Scandinavian Journal of Forest Research 19: 512–523. http://doi.org/10.1080/02827580410019463

Englhart S., Franke J., Keuck V., Siegert F. (2012). Aboveground biomass estimation of tropical peat swamp forests using SAR and optical data. IEEE International Geoscience and Remote Sensing Symposium (IGARSS), remote sensing for a dynamic earth, Munich. http://ieeexplore.ieee.org/xpl/articleDetails.jsp?arnumber=6352092. [Cited 2 Feb 2016].

Frazer G.W., Magnusson S., Wulder M.A., Niemann K.O. (2011). Simulated impact of sample plot size and co-registration error on the accuracy and uncertainty of ALS-derived estimates of forest stand biomass. Remote Sensing of Environment 115 (2): 636–649. http://doi.org/10.1016/j.rse.2010.10.008

Garcia M., Riano R., Chuvieco E., Danson F.M. (2010). Estimating biomass carbon stocks for a Mediterranean forest in central Spain using LiDAR height and intensity data. Remote Sensing of Environment 114: 816–830. http://doi.org/10.1016/j.rse.2009.11.021

Gautam B., Peuhkurinen J., Kauranne T., Gunia K., Tegel K., Latva-Käyrä P., Rana P., Eivazi A., Kolesnikov A., Hämäläinen J., Shrestha S.M., Gautam S.K., Hawkes M., Nocker U., Joshi A., Suihkonen T., Kandel P., Lohani S., Powell G., Dinerstein E., Hall D., Niles J., Joshi A., Nepal S., Manandhar U., Kandel Y., Joshi C. (2013). Estimation of Forest Carbon Using LiDAR-Assisted Multi-Source Programme (LAMP) in Nepal. In Proceedings of the International Conference on Advanced Geospatial Technologies for Sustainable Environment and Culture, Pokhara, Nepal, ISPRS Technical Commission VI, Education and Outreach, Working Group 6. p. 12–13.

Gobakken T., Korhonen L., Næsset E. (2013). Laser-assisted selection of field plots for an area-based forest inventory. Silva Fennica 47: 1–20.
http://doi.org/10.14214/sf.943

Gobakken T., Næsset E. (2008). Assessing effects of laser point density, ground sampling intensity, and field plot sample size on biophysical stand properties derived from airborne laser scanner data. Canadian Journal of Forest Research 38: 1095–1109.
http://doi.org/10.1139/X07-219

Gobakken T., Næsset E. (2009). Assessing effects of positioning errors and sample plot size on biophysical stand properties derived from airborne laser scanner data. Canadian Journal of Forest Research 39: 1036–1052.
http://doi.org/10.1139/X09-025

Gonzalez P., Asner G.P., Battles J.J., Lefsky M.A., Waring K.M., Palace M. (2010). Forest carbon densities and uncertainties from Lidar, QuickBird, and field measurements in California. Remote Sensing of Environment 114: 1561–1575.
http://doi.org/10.1016/j.rse.2010.02.011

Häme T., Rauste Y., Antropov O., Ahola H.A., Kilpi J. (2013). Improved mapping of tropical forests with optical and sar imagery, part ii: Above ground biomass estimation. IEEE Journal of Selected Topics in Applied Earth Observations and Remote Sensing 6: 92–101.
http://doi.org/10.1109/JSTARS.2013.2241020

Haralick M.R., Shanmugam K., Dinstein J. (1973). Textural features for image classification. IEEE Transactions on Systems, Man and Cybernetics 3: 610–621.
http://doi.org/10.1109/TSMC.1973.4309314

Hawbaker T.J., Keuler N.S., Lesak A.A., Gobakken T., Contrucci K., Radeloff V.C. (2009). Improved estimates of forest vegetation structure and biomass with an ALS-optimized sampling design. Journal of Geophysical Research 114: 1–11.
http://doi.org/10.1029/2008JG000870

Hou Z., Xu Q., Tokola T. (2011). Use of ALS, Airborne CIR and ALOS AVNIR-2 data for estimating tropical forest attributes in Lao PDR. ISPRS Journal of Photogrammetry and Remote Sensing 66 (6): 776–786.
http://doi.org/10.1016/j.isprsjprs.2011.09.005

Hyyppä J., Hyyppä H., Inkinen M., Engdahl M., Linko S., Zhu Y.H. (2000). Accuracy comparison of various remote sensing data sources in the retrieval of forest stand attributes. Forest Ecology and Management 128: 109–120.

IPCC (2013). Summary for policymakers. In: Stocker T.F., Qin D., Plattner G.K., Tignor M., Allen S.K., Boschung J., Nauels A., Xia Y., Bex V., Midgley P.M. (eds.) Climate change 2013: The physical science basis. Contribution of working group I to the Fifth

Assessment Report of the Intergovernmental Panel on Climate Change. Cambridge University Press, Cambridge, United Kingdom and New York, USA.

Joshi A.R., Shrestha M., Smith J.L.D., Ahearn S. (2003). Forest classification of Terai Arc Landscape (TAL) based on Landsat 7 satellite data. A final report submitted to WWF-US.

Junttila V., Finley A.O., Bradford J.B., Kauranne T. (2013). Strategies for minimizing sample size for use in airborne LiDAR-based forest inventory. Forest Ecology and Management 292: 75–85.
http://dx.doi.org/10.1016/j.foreco.2012.12.019

Junttila V., Kauranne T., Finley A.O., Bradford J.B. (2015). Linear models for airborne-laser-scanning-based operational forest inventory with small field sample size and highly correlated LiDAR data. IEEE Transactions on Geoscience and Remote Sensing 53: 5600–5612.
http://doi.org/10.1109/TGRS.2015.2425916

Junttila V., Maltamo M., Kauranne T. (2008). Sparse Bayesian estimation of forest stand characteristics from airborne laser scanning. Forest Science 54: 543–552.

Katila M., Tomppo. E. (2002). Stratification by ancillary data in multisource forest inventories employing k-nearest neighbor estimation. Canadian Journal of Forest Research 32: 1548–1561.
http://doi.org/10.1139/X02-047

Kaufman Y.J., Tanre D. (1996). Strategy for direct and indirect methods for correcting the aerosol effect on remote sensing: From AVHRR to EOS-MODIS. Remote Sensing of Environment 55: 65–79.
http://dx.doi.org/10.1016/0034-4257(95)00193-X

Khosravipour A., Skidmore A.K., Wang T., Isenburg M., Khoshelham K. (2015). Effect of slope on treetop detection using a LiDAR Canopy Height Model. ISPRS Journal of Photogrammetry and Remote Sensing 104: 44–52.
http://doi.org/10.1016/j.isprsjprs.2015.02.013

Koch B. (2010). Status and future of laser scanning, synthetic aperture radar and hyper-spectral remote sensing data for forest biomass assessment. ISPRS Journal of Photogrammetry and Remote Sensing 65: 581–590.
http://doi.org/10.1016/j.isprsjprs.2010.09.001

Köhl M., Magnussen S., Marchetti M. (2006). Sampling methods, remote sensing and GIS multisource forest inventory. Springer-Verlag, Berlin Heidelberg. 373 p.
http://dx.doi.org/10.1007/978-3-540-32572-7

Korf V. (1939). Prispevek k matematicke definici vzrus-toveho zakona hmot lesnich porostu. Lesnicka pracr 18: 339–379.

Korhonen L., Peuhkurinen J., Malinen J., Suvanto A., Malatamo M., Packalén P., Kangas J. (2008). The use of airborne laser scanning to estimate sawlog volumes. Forestry 81: 499–510.
http://doi.org/10.1093/forestry/cpn018

Korpela I., Ørka H.O., Hyyppä J., Heikkinen V., Tokola T. (2010). Range and AGC normalization in airborne discrete-return LiDAR intensity data for forest canopies. ISPRS Journal of Photogrammetry and Remote Sensing 65: 369–379.
http://doi.org/10.1016/j.isprsjprs.2010.04.003

Laasasenaho J. (1982). Taper curve and volume function for pine, spruce and birch. Communicationes Instituti Forestalis Fenniae 108: 1–74.

Latifi H., Nothdurft A., Koch B. (2010). Non-parametric prediction and mapping of standing timber volume and biomass in a temperate forest: Application of multiple optical/LiDAR-derived predictors. Forestry 83: 395–407.
http://doi.org/10.1093/forestry/cpq022

Laurin G.V., Chen Q., Lindsell J.A., Coomes D.A., Frate F.D., Guerriero L., Pirotti F., Valentini R. (2014). Above ground biomass estimation in an African tropical forest with lidar and hyperspectral data. ISPRS Journal of Photogrammetry and Remote Sensing 89: 49–58.
http://doi.org/10.1016/j.isprsjprs.2014.01.001

Lefsky M.A., Cohen W.B., Harding D.J., Parker G.G., Acker S.A., Gower S.T. (2002a). LiDAR remote sensing of above-ground biomass in three biomes. Global Ecology and Biogeography 11: 393–399.
http://doi.org/10.1046/j.1466-822x.2002.00303.x

Lefsky M.A., Cohen W.B., Parker G.G., Harding D.J. (2002b) Lidar remote sensing for ecosystem studies. BioScience 52: 19–30.
http://doi.org/10.1641/0006-3568(2002)052[0019:LRSFES]2.0.CO;2

LeMay V., Temesgen H. (2005). Comparison of nearest neighbor methods for estimating basal area and stems per hectare using aerial auxiliary variables. Forest Science 51: 109–119.

Lu D., Chen Q., Wang G., Liu L., Li G., Moran E. (2016). A survey of remote sensing-based aboveground biomass estimation methods in forest ecosystems. International Journal of Digital Earth 9: 63–105.
http://doi.org/10.1080/17538947.2014.990526

Lu D. (2006). The potential and challenge of remote sensing-based biomass estimation. International Journal of Remote Sensing 27: 1297–1328.
http://doi.org/10.1080/01431160500486732

Maltamo M., Bollandsas O.M., Næsset E., Gobakken T., Packalén P. (2011). Different plot selection strategies for field training data in ALS-assisted forest inventory. Forestry 84: 23–31.
http://doi.org/10.1093/forestry/cpq039

Mascaro J., Asner G.P., Muller-Landau H.C., Van Breugel M., Hall J., Dahlin K. (2011). Controls over aboveground forest carbon density on Barro Colorado Island, Panama. Biogeosciences 8: 1615–1629.
http://doi.org/10.5194/bg-8-1615-2011

Merger E., Held C., Tennigkeit T., Blomley T. (2012). A bottom-up approach to estimating cost elements of REDD+ pilot projects in Tanzania. Carbon Balance and Management 7: 1–14.
http://doi.org/10.1186/1750-0680-7-9

Moeur M., Stage A.R. (1995). Most similar neighbour: an improved sampling inference procedure for natural resource planning. Forest Science 41: 337–359.

Montgomery D.C., Peck E.A., Vining G.G. (2006). Introduction to Linear Regression Analysis. Wiley-Interscience, Hoboken, New Jersey. 640 p.

Morsdorf F., Nichol C., Malthus T., Woodhouse I.H. (2009). Assessing forest structural and physiological information content of multi-spectral LiDAR waveforms by radiative transfer modelling. Remote Sensing of Environment 113: 2152–2163.
http://doi.org/10.1016/j.rse.2009.05.019

Murdiyarso D., Skutsch M. (2006). Promoting Carbon Benefits from Community Forest Management. In: Murdiyarso D., Skutsch M. (eds.) Community Forest Management as a carbon mitigation option. Centre for International Forestry Research (CIFOR), Bogor, Indonesia. p. 1–7.

Næsset E. (2002). Predicting forest stand characteristics with airborne scanning laser using a practical two-stage procedure and field data. Remote Sensing of Environment 80: 88–99.
http://doi.org/10.1016/S0034-4257(01)00290-5

Næsset E., Bollandsås, O.M., Gobakken, T. (2005). Comparing regression methods in estimation of biophysical properties of forest stands from two different inventories using laser scanner data. Remote Sensing of Environment 94: 541–553.
http://doi.org/10.1016/j.rse.2004.11.010

Næsset E., Ørka H.O., Solberg S., Bollandsås O.M., Hansen E.H., Mauya E., Zahabu E., Malimbwi R., Chamuya N., Olsson H., Gobakken T. (2016). Mapping and estimating forest area and aboveground biomass in miombo woodlands in Tanzania using data from airborne laser scanning, TanDEM-X, RapidEye, and global forest maps: A comparison of estimated precision. Remote Sensing of Environment 175: 282–300.
http://doi.org/10.1016/j.rse.2016.01.006

Näslund M. (1936). Skogsförsöksanstaltens gallringsförsök i tallskog. Meddelanden från Statens Skogsförsöksanstalt 29: 169. [In Swedish with English summary].

Norjamäki I., Tokola T. (2007). Comparison of Atmospheric Correction Methods in Mapping Timber Volume with Multitemporal Landsat Images in Kainuu, Finland. Photogrammetric Engineering & Remote Sensing 73: 155–163. http://doi.org/10.14358/PERS.73.2.155

Olofsson P., Foody G.M., Herold M., Stehman S.V., Woodcock C.E., Wulder M.A. (2014). Good practices for estimating area and assessing accuracy of land change. Remote Sensing of Environment 148: 42–57. http://doi.org/10.1016/j.rse.2014.02.015

Packalén P., Maltamo M. (2007). The k-MSN method for the prediction of species specific stand attributes using airborne laser scanning and aerial photographs. Remote Sensing of Environment 109: 328–341. http://doi.org/10.1016/j.rse.2007.01.005

Packalén P., Maltamo M., Tokola T. (2008). Detailed assessment using remote sensing techniques. In: Von G.K., Pukkala I. (eds.) Designing Green Landscapes: Managing Forest Ecosystems. Springer, Netherlands. p. 53–77.

Packalén P., Suvanto A., Maltamo M. (2009). A Two Stage Method to Estimate Species-specific Growing Stock. Photogrammetric Engineering & Remote Sensing 75: 1451–1460. http://doi.org/10.14358/PERS.75.12.1451

Packalen P., Temesgen H., Maltamo M. (2012). Variable selection strategies for nearest neighbor imputation methods used in remote sensing based forest inventory. Canadian Journal of Remote Sensing 38: 557–569.

Pan Y, Birdsey R.A., Fang J., Houghton R., Kauppi P.E., Kurz W.A., Phillips O.L., Shvidenko A., Lewis, S.L., Canadell J.G., et al. (2011). A large and persistent carbon sink in the world's forests. Science 333: 988–993. http://doi.org/10.1126/science.1201609

Pant P., Heikkinen V., Hovi A., Korpela I., Hauta-Kasari M., Tokola T. (2013). Evaluation of simulated bands in airborne optical sensors for tree species identification. Remote Sensing of Environment 138: 27–37. http://doi.org/10.1016/j.rse.2013.07.016

Pariyar D. (1998). Country pasture/forage resource profiles Nepal. Pasture and Fodder Research Division, Khumaltar, Post Box 11660, Kathmandu, Nepal. Published by Food and Agriculture Organization, Italy. http://www.fao.org/ag/agp/agpc/doc/counprof/nepal.htm#1 [Cited 25 Jan 2016].

Penner M., Pitt D.G., Woods M.E. (2013). Parametric vs. nonparametric LiDAR models for operational forest inventory in boreal Ontario. Canadian Journal of Remote Sensing 39: 426–443.
http://doi.org/10.5589/m13-049

RapidEye (2012). RapidEye - Delivering the world.
http://www.rapideye.de. [Cited 01 Feb 2012].

Repola J. (2008). Biomass equations for birch in Finland. Silva Fennica 42: 605–624.

Repola J. (2009). Biomass equations for scots pine and norway spruce in Finland. Silva Fennica 43: 625–647.

Sharma E.R., Pukkala T. (1990). Volume equations and biomass prediction of forest trees of Nepal. Forest Survey and Statistics Division, Ministry of Forests and Soil Conservation. Babar Mahal, Kathmandu, Nepal. Publication 47, pp. 1–16.

Song C., Woodcock C.E., Seto K.C., Lenney M.P., Macomber S.A. (2001). Classification and change detection using Landsat TM data: When and how to correct atmospheric effects? Remote Sensing of Environment 75: 230–244.
http://doi.org/10.1016/S0034-4257(00)00169-3

Streck C., Scholz S.M. (2006). The role of forests in global climate change: Whence we come and where we go. International Affairs 82: 861–879.
http://doi.org/10.1111/j.1468-2346.2006.00575.x

Tamura H., Mori S., Yamawaki T. (1978). Textural features corresponding to visual perception. IEEE Transactions on Systems, Man and Cybernetics 8: 460–472.
http://doi.org/10.1109/TSMC.1978.4309999

Temesgen H. (2003). Estimating stand tables from aerial attributes: a comparison of parametric prediction and most similar neighbour methods. Scandinavian Journal of Forest Research 18: 279–288.
http://doi.org/10.1080/02827581.2003.9728298

Tian X., Su Z., Chen E., Li Z., Tol C., Guo J., He Q. (2012). Estimation of forest above-ground biomass using multi-parameter remote sensing data over a cold and arid area. International Journal of Applied Earth Observation and Geoinformation 14: 160–168.
http://doi.org/10.1016/j.jag.2011.09.010

Tokola T. (2015). Remote Sensing Concepts and Their Applicability in REDD+ Monitoring. Current Forestry Reports 1: 252–260.
http://doi.org/10.1007/s40725-015-0026-4

Tokola T., Hou Z. (2012). Alternative remote sensing materials and inventory strategies in tropical forest inventory - case Lao PDR. Ambiência 8: 483–500.
http://doi.org/10.5777/ambiencia.2012.04.04

Tokola T., Löfman S., Erkkilä A. (1999). Relative calibration of multitemporal landsat data for forest cover change detection. Remote Sensing of Environment 68: 1–11. http://doi.org/10.1016/S0034-4257(98)00096-0

Tokola T., Shrestha S.M. (1999). Comparison of cluster-sampling techniques for forest inventory in southern Nepal. Forest Ecology and Management 116: 219–231. http://doi.org/10.1016/S0378-1127(98)00457-5

Tuia D., Ratle F., Pacifici F., Kanevski M.F., Emery W.J. (2009). Active Learning Methods for Remote Sensing Image Classification. IEEE Transactions on Geoscience and Remote Sensing 47: 2218–2232. http://doi.org/10.1109/TGRS.2008.2010404

Tuominen S., Pekkarinen A. (2004). Local radiometric correction of digital aerial photographs for multi source forest inventory. Remote Sensing of Environment 89: 72–82. http://doi.org/10.1016/j.rse.2003.10.005

Tuominen S., Pekkarinen A. (2005). Performance of different spectral and textural aerial photograph features in multi-source forest inventory. Remote Sensing of Environment 94: 256–268. http://doi.org/10.1016/j.rse.2004.10.001

UNFCCC (2009). Decision on methodological guidance for activities relating to reduced emissions from deforestation and forest degradation and the role of conservation, sustainable management of forests and enhancement of forest carbon stocks in developing countries. Draft decision -/CP.15 Bonn, June 2009. http://unfccc.int/files/na/application/pdf/cop15_ddc_auv.pdf [cited May 21, 2016].

U.S. Geological Survey (2012). Landsat processing details. http://landsat.usgs.gov/Landsat_Processing_Details.php. [Cited 01 Aug 2012].

Vauhkonen J., Korpela I., Maltamo M., Tokola T. (2010). Imputation of single-tree attributes using airborne laser scanning-based height, intensity and alpha shape metrics. Remote Sensing of Environment 114: 1263–1276. http://doi.org/10.1016/j.rse.2010.01.016

Vauhkonen J., Næsset, E., Gobakken T. (2014). Deriving airborne laser scanning based computational canopy volume for forest biomass and allometry studies. ISPRS Journal of Photogrammetry and Remote Sensing 96: 57–66. http://doi.org/10.1016/j.isprsjprs.2014.07.001

Walker W.S., Kellndorfer J.M., LaPoint E., Hoppus M., Westfall J. (2007). An Empirical InSAR-optical Fusion Approach to Mapping Vegetation Canopy Height. Remote Sensing of Environment 109: 482–499. http://doi.org/10.1016/j.rse.2007.02.001.

Wertz-Kannounnikoff S. (2008). Estimating the costs of reducing forest emissions – A review of methods. Center for International Forestry Research (CIFOR) Working Paper No. 42. Bogor, Indonesia.

White D., Minang P. (2011). Estimating the opportunity costs of REDD+: A training manual. Alternatives to Slash-and-Burn (ASB) and The World Bank Institute. 257 p.

White J.C., Stepper C., Tompalski P., Coops N.C., Wulder M.A. (2015). Comparing ALS and image-based point cloud metrics and modelled forest inventory attributes in a complex coastal forest environment. Forests 6: 3704–3732. http://doi.org/10.3390/f6103704

Woodhouse I.H., Nichol C., Sinclair P., Jack J., Morsdorf F., Malthus T.J., Patenaude G. (2011). A Multispectral Canopy LiDAR Demonstrator Project IEEE Geoscience and Remote Sensing Letters 8: 839–843. http://doi.org/10.1109/LGRS.2011.2113312

Wulder M., White J.C., Bater C.W., Coops N.C., Hopkinson C., Chen G. (2012). Lidar plots — a new large-area data collection option: context, concepts, and case study. Canadian Journal of Remote Sensing 38: 600–618. http://doi.org/10.5589/m12-049

Xu Q., Hou Z., Tokola T. (2012). Relative radiometric correction of multi-temporal ALOS AVNIR-2 data for the estimation of forest attributes. ISPRS Journal of Photogrammetry and Remote Sensing 68: 69–78. http://doi.org/10.1016/j.isprsjprs.2011.12.008

Zahabu E. (2008) A strategy to involve forest communities in Tanzania in global climate change policy. PhD Dissertation, University of Twente.

Zhao K., Popescu S., Nelson R. (2009). Lidar remote sensing of forest biomass: a scale-invariant estimation approach using airborne lasers. Remote Sensing of Environment 113: 182–196. http://doi.org/10.1016/j.rse.2008.09.009

Zolkos S.G., Goetz S.J., Dubayah R. (2013). A meta-analysis of terrestrial aboveground biomass estimation using lidar remote sensing. Remote Sensing of Environment 128: 289–298. http://doi.org/10.1016/j.rse.2012.10.017